Graduate Theses and Dissertations

Graduate School

January 2012

Assessment of Methods to Manipulate Thermal Emission and Evaluate the Quality of Thermal Radiation for Direct Energy Conversion

Samantha Wijewardane
University of South Florida, swijewar@mail.usf.edu

Assessment of Methods to Manipulate Thermal Emission and

Evaluate the Quality of Thermal Radiation for Direct Energy Conversion

by

Samantha Wijewardane

A dissertation submitted in partial fulfillment
of the requirements for the degree of
Doctor of Philosophy
Department of Chemical and Biomedical Engineering
College of Engineering
University of South Florida

Major Professor: Yogi D Goswami, Ph.D.
Elias Stefanakos, Ph.D.
Amir Abtahi, Ph.D.
Babu Joseph, Ph.D.
Muhammad Rahman, Ph.D.

Date of Approval:
November 19, 2012

Keywords: Exergy, Surface Plasmon, Mutual Intensity, Degree of Coherence,
Rectenna

ACKNOWLEDGMENTS

TABLE OF CONTENTS

LIST OF TABLES

LIST OF FIGURES

ABSTRACT

Control of spectral thermal emission from surfaces may be desirable in some energy related applications, such as nano-scale antenna energy conversion and thermophotovoltaic conversion. There are a number of methods, from commercially available paints to advanced surface gratings that can be used to modify the thermal emission from a surface. To find out the proper emission controlling technique for a given energy conversion method all the surface emission controlling methods are comprehensively reviewed regarding the emission control capabilities and the range of possible applications. Radiation with high degree of coherence can be emitted using advanced surface emission controlling techniques. The entropy of the thermal radiation, and therefore the exergy, is a function of the degree of coherence. A methodology is presented to calculate the exergy of partially coherent wave fields so that the radiation fields can be evaluated based on exergy. This exergy method is extended to develop a rigorous evaluation criterion for thermal emission controlling methods used in frequency dependent energy conversion applications. To demonstrate these developed criteria using actual data, a surface plasmon emitter is designed and fabricated. Also, possible ways of improving the emitter performance and the research needed to be carryout to fabricate cost effective emitters are described.

1. INTRODUCTION

Control of spectral thermal emission from surfaces may be needed in some applications, such as nano-scale antenna energy conversion and thermophotovoltaic conversion. Radiation from a surface can be controlled spectrally and spatially and the polarization and coherence of the radiation field can be modified. There are a number of methods, from commercially available paints to advanced surface gratings, which can modify the thermal emission from a surface. These methods have their own capabilities and limitations and can be used for a variety of applications. Thermophotovoltaics and the emerging "Rectenna" (rectifying antenna) technology are direct conversion techniques that have gained attention over the past few years because of their anticipated high efficiency and the clean electric conversion. Although high efficiency is predicted from these devices, they have their own limitations which are bounded by the spectrum and/or the quality of the radiation. For example not all of the energy of a random radiation is usable for nanoscale antenna devices. Therefore, to achieve high efficiency, the nano rectenna devices require radiation with acceptable polarization and a high degree of coherence within an acceptable spectral range. Similarly thermophotovoltaic systems require radiation with frequencies just above the cut off frequency of the photo cell.

Because of the large number of methods that can be used to control thermal emission from a surface, it is an intricate task to identify the most effective emission controlling technique for a given energy conversion method, that exhibits the desired radiation properties for high energy conversion efficiency. There are, however, some

1

promising emerging technologies that can be used to control spectral emission. The development of these techniques is at a nascent level, and, thus, it is a difficult task to integrate these technologies to simultaneously achieve high efficiency and reasonable cost. Therefore, there is a need for a thorough assessment of spectral controlling techniques that takes into consideration all aspects of the energy conversion method. In the next section we provide in depth analysis of the problem by dividing it into smaller parts. In the sections after that we elaborate on: (a) the solutions to the problems, (b) the details of the design and fabrication of a surface plasmon emitter which can be used to demonstrate the evaluation criteria, and (c) an description of future work that can be carried out in order to improve the emitter performance.

2

2. THE NECESSITIES FOR THE ASSESSMENT OF THERMAL EMISSION

2.1 The Need for a Review of Thermal Emitting Techniques and Applications

There is a variety of surface emission controlling methods ranging from paints to advanced surface gratings which vary in terms of economics, technologies, availability, durability as well as applicable temperature range. Thus, there is a need for a comprehensive review of thermal emitting techniques, their emission controlling capabilities and the range of possible applications.

2.2 The Need to Develop a Methodology to Evaluate Thermal Emitters

There is a need to evaluate these emitters based on their ability to provide "usable" energy for a given conversion method, and it requires the development of some new concepts. The lack of an appropriate methodology for the evaluation of thermal radiation emitters used in energy conversion systems is highlighted by many researchers [1]. Emitter properties such as emissivity, spectral characteristics, directivity or collimation are commonly used for evaluation purposes; however, these properties are not adequate for some energy conversion processes. Since different conversion methods have specific requirements for the conversion of incident radiation, the emitters must be evaluated based on their ability to meet the specific requirements of each conversion method. Farfan et al [2] has defined the energetic emitter efficiency as the ratio of the energy emitted in the band of interest (or desired emission window) to the overall energy emitted (Figure 1).
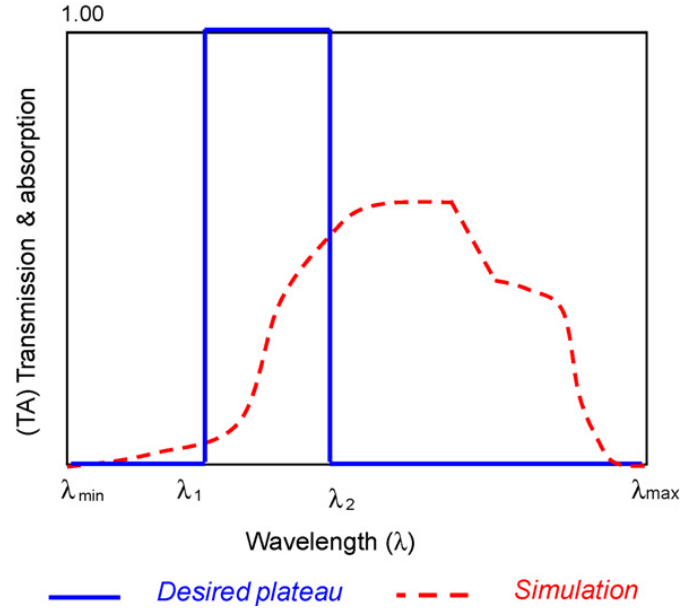
Figure 1. A schematic representation of the desired TA plateau Vs the simulated profile for an arbitrary emitted radiation [2].

Hence, referring to the figure, the emitter efficiency (η_e) is defined as

$$\eta_e = \frac{\int_{\lambda_1}^{\lambda_2} TA(\lambda) N_E(\lambda)}{\int_{\lambda_{min}}^{\lambda_{max}} TA(\lambda) N_E(\lambda)} \tag{1}$$

Here $TA(\lambda)$ is the combined transmissivity and absorptivity (absorptivity equals emissivity) of the emitter and $N_E(\lambda)$ is the blackbody emission at λ. The transmission through the emitter is also considered to account for the total radiation flux (transmission and emission) through the emitter. The band of interest depends on the ability of the converting mechanism in which this emitter is to be employed. This is the only definition for the efficiency of thermal selective emitters in the literature so far but even this definition has a basic shortcoming as explained below. In a photovoltaic (PV) cell the "wavelength band of interest" is from zero to its cutoff wavelength, based on its band gap. At least part of the radiation energy within this frequency range can be converted to electricity, although the energy of the photons in excess of the band gap is wasted as heat by a thermalization process instead of being converted to electric power. The photons at the cutoff wavelength could be converted

4

at the maximum efficiency, while photons at lower wavelengths would be converted at a lower efficiency. Figure 2 shows this scenario schematically. Curve A is the profile of blackbody radiation at temperature T incident on a PV cell. The hatched area represents the electric power that could be converted in the cell after removing the wasted energy due to the thermalization process.
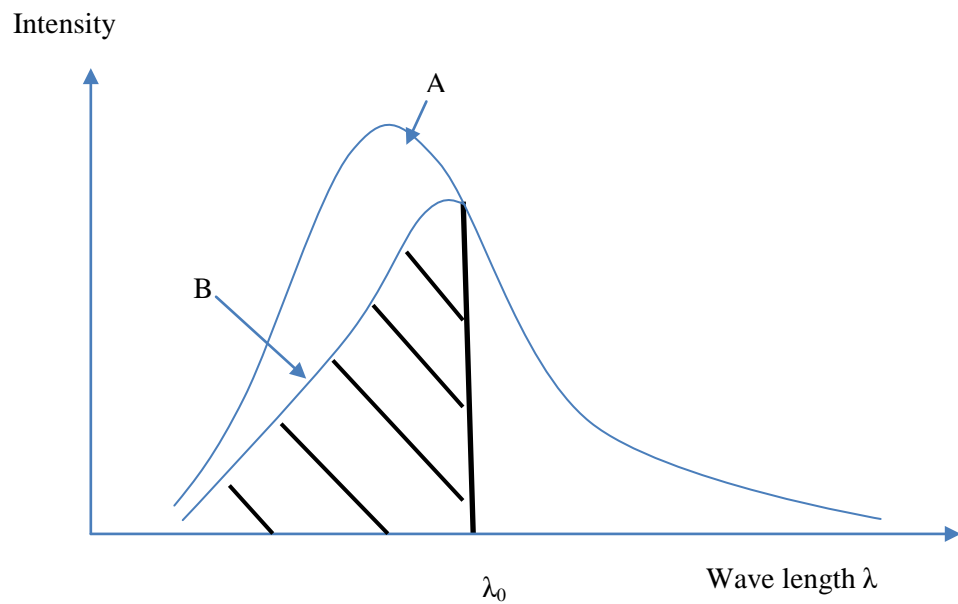
Figure 2. Energy conversion from a photocell with a cutoff wavelength λ_0

Now, consider two spectral profiles, 1 and 2, as shown in figure 3, from two different emitters incident on this cell instead of the blackbody radiation. If we assume the total energy emitted is the same in each case, then, according to equation 1, these two emitters have the same energy efficiency which is equal to unity. However the emitter profile 2 which has more excess energy than the emitter profile 1 will produce less power in a PV cell and therefore the emitter 1 is superior to 2 when they are used in this particular application. Therefore, the Farfan definition fails to distinguish the performances of these emitters used in thermophotovoltaic applications. This implies that the definition of emitter efficiency should consider the

5

intrinsic capabilities of the conversion mechanism in which these emitters are to be employed. In other words we have to consider the usability of the emitted radiation with respect to the conversion mechanism in order to evaluate their performances in an explicit manner. Therefore the thermodynamic "exergy" method may be the most appropriate way of analyzing the emitter performances.
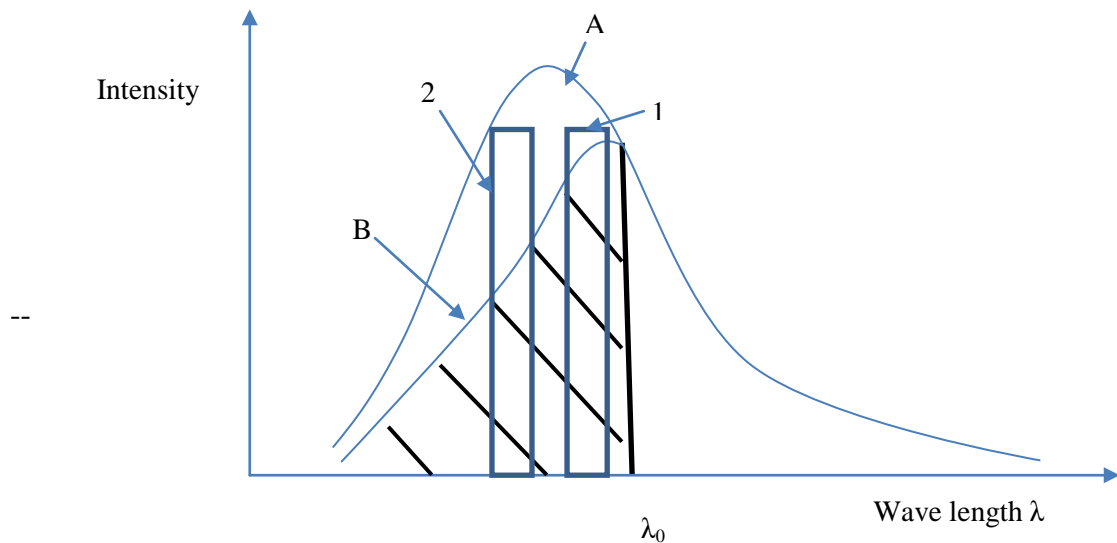
Figure 3. The spectral profiles of two emitters (1 and 2) which could be used to replace the blackbody in figure 2.

In part 2 of the solution section we have described the derivation of a new evaluation criterion which is more appropriate than the equation 1 and also the usability of this new evaluation criterion.

2.3 Lack of a Method to Calculate Exergy of Partially Coherent Thermal Radiation

The evaluation criterion proposed in the previous section needs the exergy of thermal radiation as an input. In general coherence is the ability of the wave field to interfere stationary either temporally or spatially. The radiation from the real sources is partially coherent and frequency selective thermal emitters can emit radiation with high degree of coherence. Degree of coherence is a critical factor that affects the entropy and thereby the exergy of the radiation field. Therefore we need to calculate

6

the exergy of partially coherent thermal radiation. Although the exergy of electromagnetic radiation has been studied by a number of researchers for well over four decades none of them paid attention to the partial coherent properties of thermal radiation, because these researchers primarily dealt with solar and blackbody radiation which has a low degree of coherence. So in the section 3.3 we demonstrate a method to calculate exergy of partially coherent thermal radiation.

7

3. ASSESSMENT OF THERMAL EMISSION

3.1 Review of Thermal Emitting Techniques and Applications

We have comprehensively reviewed surface emission controlling methods regarding the emission control capabilities and the range of possible applications. First we focused on paints and coatings, which, in many ways, are different from other methods of emission control, such as, limitations of spectral control, involved technologies, economics and possible applications. Then we reviewed more advanced types of thermal emission controlling mechanisms, such as, surface plasmon gratings and other photonic structures to find out the possible ways of improving their performances to suit the energy applications. In the paint and coatings review we presented a brief but effective criterion for the formation of spectrally selective paints for energy applications. Also we discussed present and possible future research opportunities to optimize these coatings and paints for spectral selectivity for specific applications. Those findings are presented in next two sections. The finding[1]s of the literature search for more advanced types of thermal emission controlling mechanisms, i.e. possible ways of improving their performances to suit the energy applications, are presented in chapter 5.

3.1.1 A Brief Criterion for Selective Paint Formation

Spectrally controlling thermal emission has many advantages. Here a brief criterion is presented to design paint coatings for a given range of the spectrum. Paint represents a complex multicomponent system. In most cases, the individual

---

[1] Part of these materials are taken from the previous published articles [34,35] and the license agreement can be found in Appendix 3.

components, i.e. binder, solvent and pigment, are also of complex combination. The optical performance of a coating depends upon the properties of the substrate: paint layer thickness; complex refractive index of the matrix (resin); properties of scattering particles; complex refractive index; average size; volume fraction; degree of dispersion; and distribution across the layer [3]. Therefore the inverse calculation, i.e finding the combination of pigments and pigment sizes for a given selective emission by calculation is almost impossible. However, there is a vast literature on spectral selectivity for many applications, such as camouflage coatings, fire protection coatings, and solar thermal applications, which represent a wide span of frequency range. Therefore it is possible to acquire much vital information such as pigment types and resin types to start designing paint with a custom selectivity. In appendix 1 we tabulated the optical properties of pigments, resins and solvents. The most important factor is the composition of the constituents. Also it is essential to think about the method of application and the distribution of particles in the final dry coating, which strongly defines the final optical properties.

If paint is always applied on the same substrate then the optical properties of this substrate can be effectively used to obtain the required selectivity by combining the optical properties of the paint layer with those of the substrate. This is the method used in TSSS paints. On the other hand, if paint is to be applied on different types of surfaces then the paint layer must provide the required selectivity by itself and should avoid any "see through" effect of the substrate. These types of paints can be applied not only on any type of substrate but also on any arbitrarily shaped object, as there is no need for controlling the thickness as in the TSSS paints.

To determine the type of pigments and resins to start with, the following approximate procedure can be applied. For the frequency range in which high

reflectivity is desired, the scattering coefficient of the paint should high. The scattering coefficient depends on the mutual effect of the optical properties of the constituents of paint film and it can be taken approximately as the ratio of the refractive indices of the pigment and the resin. The absorption of the paint layer largely depends on the intrinsic absorptivity of the pigment type. That means within the frequency range in which high reflectivity is desired, the imaginary (absorptive) part of the refractive index of the pigment should have a small value, and if high absorptivity or emissivity is preferred for some other frequency range, the pigment(s) should possess high absorption for that particular range. To achieve the selectivity between different spectral ranges it may be required to use a second pigment type as an extended pigment or filler but the incorporation of additional constituents always complicates the process and therefore should be avoided. Also pigments can be tailor-made to provide the required selective properties. One such pigment used in solar thermal applications is prepared by coating a thin layer of an appropriate black oxide to a highly reflecting metallic particle so that the combined pigment characterizes an absorber/ reflector tandem as in TSSS paints. Although the absorption by the binder or resin could be neglected at the initial lay-out of the design most organic resins exhibit some absorption in the mid infrared range. A qualitative discussion on this issue can be found in [4].

Possible combinations of pigment types and resins can be found in the literature for the desired range of frequencies considering the above scenarios. The number of possible pigment types and resins can be further reduced by screening with respect to the environmental issues, durability, stability, and chalking effect. Once possible types of pigments are identified, the size (s) of pigments can be calculated from the following approximate method. For a fixed value of scattering

power "*m*" the wave length λ that is most efficiently scattered by a particle of diameter "*d*" is given by [5].

$$\frac{d}{k} = \lambda$$

(2)

In which

$$\frac{0.9(m^2 + 2)}{n\pi(m^2 - 1)} = k$$

(3)

where *n* is the refractive index of the resin.

Using these equations, the particle diameter *d* that could effectively scatter the mean of the desired frequency range can be calculated. It is important to note that this should be the diameter of the particles in the paint system, which might be different from the sizes of the commercially available particles due to the aggregates and agglomerates that are always present in the paint system. The sizes of these agglomerate particles can be reduced by paint dispersion techniques such as mechanical milling, but these processes are highly energy Intensive.

After gathering the required information such as resin types, pigment types and their sizes, a more rigorous calculation method can be used to optimize these parameters and to find other important parameters. With the advancement in the computer simulation, it is quite possible to model a detailed description of the potential paint layer with all the vital parameters. Optimizing the parameters by doing a complex and realistic calculation at this stage will reduce the number of costly repetitions at the testing stage, thereby reducing the overall cost involved in the paint development phase. Even though it is hard to include the effects of shapes and orientation of the agglomerate particles, there are some attempts [6] to find the light scattering properties of rutile particles with different characteristic morphological shapes using the finite-element method. Depending on the simulation results,

parameters can be optimized using an iterative method. Changing the simulation parameters, such as, particle sizes and pigment-to-volume concentration (PVC) is vital and saves time. When PVC and thickness of the layer increases, the absorption coefficient and scattering coefficient values are normally expected to be higher because of the availability of more particles in which absorption and scattering can take place. When the mean particle size of the pigment accumulation increases, the longer radiation tends to scatter more effectively. Deviations from these scenarios are quite possible due to the high complexity of paint constituents.

After optimizing all the important parameters the paint should be formed and tested. The particle size is important for the optical properties and in general particle sizes in frequency-selective paints are larger than in normal commercial paints. In practice the dispersion will not be perfect and standard deviation of particle sizes could be different than anticipated. So there is no substitute for experiments and testing to find out the real picture. Determining the degree of dispersion in the dry paint film is vital for improvements. There are many techniques, such as, electron microscopy, light scattering method and flocculation gradient to find the degree of dispersion [7]. Based on the experimental results the parameters could be changed to obtain the desired selectivity as closely as possible. Optimization largely depends on how well the parameters can be controlled in the experiment.

3.1.2 Achieving the Narrow Spectral Selectivity Using Paints

In conventional applications, such as solar thermal and radiative cooling, the spectral selectivity of paints and coatings has been achieved close to the ideal because of intensive research pursued over the last 50 years. However, achieving a narrow band spectral selectivity by paints or coatings is still a challenge. Achieving the required selectivity using paints or coatings would have a huge impact due to their

12

cost effectiveness and ease of application, compared to other available technologies for narrow band selectivity. Here we discuss recent efforts to achieve narrow band selectivity, the current challenges and the possible directions of research that should be taken. To change the spectral reflectance or emission and to obtain the required selectivity, the optical properties of the paints or coatings must be modified. The most important optical properties to achieve this task are absorption coefficient, scattering coefficient and in some cases, where interference is employed for selectivity, the refractive index. To use a narrower selectivity using the scattering effect, the paint or coating should have a scattering coefficient that has a peak or minimum depending on the application with respect to the frequency in the vicinity of the targeted frequency. The scattering of visible and infrared radiation by a pigment is approximately a linear function of the difference between the refractive indices of the pigment and the resin. So, to have the required selectivity, the difference of refractive indices should have a maximum or a minimum with respect to the frequency. It is hard to find materials with such characteristics in nature, but there is a possibility to create such matter with the help of nanotechnology.

For a fixed value of scattering power "*m*" the wave length λ that is most efficiently scattered by a particle of diameter "*d*" is given by equation 2. The scattering power *m* of a pigment for white light is defined as the ratio between the refractive index of the pigment and the resin. Here, as in equation 3, for a fixed refractive index *n* the relationship of the particle size and wave length is linear. This means that for a particular size, particles will scatter other wavelengths in the vicinity of the wave length of interest with almost the same efficiency as they would scatter the wavelength of interest itself. Also in practice it is not possible to regulate an exact particle size; a distribution of particle sizes with the mean equal to the required size is

what one gets even from the best techniques. Therefore these distributions of particle sizes could effectively scatter the corresponding wavelengths according to equation 9, resulting in a dampened spectral peak. This is a disadvantage of paints and coatings where particles are an intrinsic constituent. The effect of the absorption coefficient on the selectivity is straight forward. A frequency-dependent absorption coefficient with the peak at a required frequency will result in a peak emissivity at that frequency. There are many materials that have absorption peaks at different wave lengths. Rare earth metals can be used as selective emitters in the infrared region due to their high absorption in this region [7]. Commonly, these metals are used as composites by mixing with other materials such as ceramic or titania because of the unavailability of these metals. The problem with these composites is that at higher temperatures grey-body like emission from other constituents' starts to dominate the rare earth metal's selective emission (figures 4 and 5).

For applications which require peaks of various wavelengths, the absorption peaks have to be tuned or shifted and the answer again falls in the nano scale. The thin coatings that use the interference phenomena for spectral selectivity have their thickness controlled depending on the refractive index of the film and the surroundings to obtain the required spectral peaks. A rapid change of refractive index with the frequency in the vicinity of the frequency of interest will enhance the selectivity. Here a peak of the refractive index at the frequency of interest is not a necessity. Nanosized metals and semiconductor particles show novel physical properties which are related to both classical and quantum size effects. Nano-composite materials consisting of metal or semiconductor particles embedded in various matrices have been of interest for a long time due to their tunable optical and physical properties. A large amount of research has been done on nanocomposite

14

materials in which nanosized metal particles are embedded in insulators, while several investigations have also been carried out on metal particles embedded in a semiconductor matrix. At a low concentration of nano metal particles, the properties of the composites are almost similar to the properties of the host matrix, either insulator (ceramic) or semiconductor (Si), while by increasing the metal content the properties start to deviate more and more from the host materials. At a certain concentration of metal particles (known as the percolation limit) the composite properties start to show the properties of the bulk metal. This concentration range, where composite properties are changing from insulator/ semiconductor properties to bulk metal properties, is known as the transition range. At this range, composites show some interesting optical properties such as peak absorptions at particular frequencies, and sudden step-up of the refractive index, which are not present in the bulk form of either material. These changes of optical properties, such as absorption resonance, can be qualitatively explained by resonant oscillations of surface charges in the electromagnetic field.

The possibility of tuning the optical properties at this transition range to suit particular applications has attracted the interest of many researchers. As shown in the graph (Fig. 7) a peak of extinction coefficient at a wavelength of 550 nm has appeared in the composite of Au and amorphous carbon [9]. The peak starts to further develop and shifts slightly towards the higher wavelengths with the increase of metal concentration up to the percolation limit. Also a step in the refractive index can be seen from 500-700 nm (Fig. 6). This sudden incremental change in the refractive index can be utilized well to develop a thin coating with a sharp reflectance minimum in the vicinity of 600 nm, i.e. in between 500 to 700 nm. A nano composite made

from Si-Ag with a co-sputtering technique shows a strong absorption peak at 610 nm with 40% Ag nano particles [10].
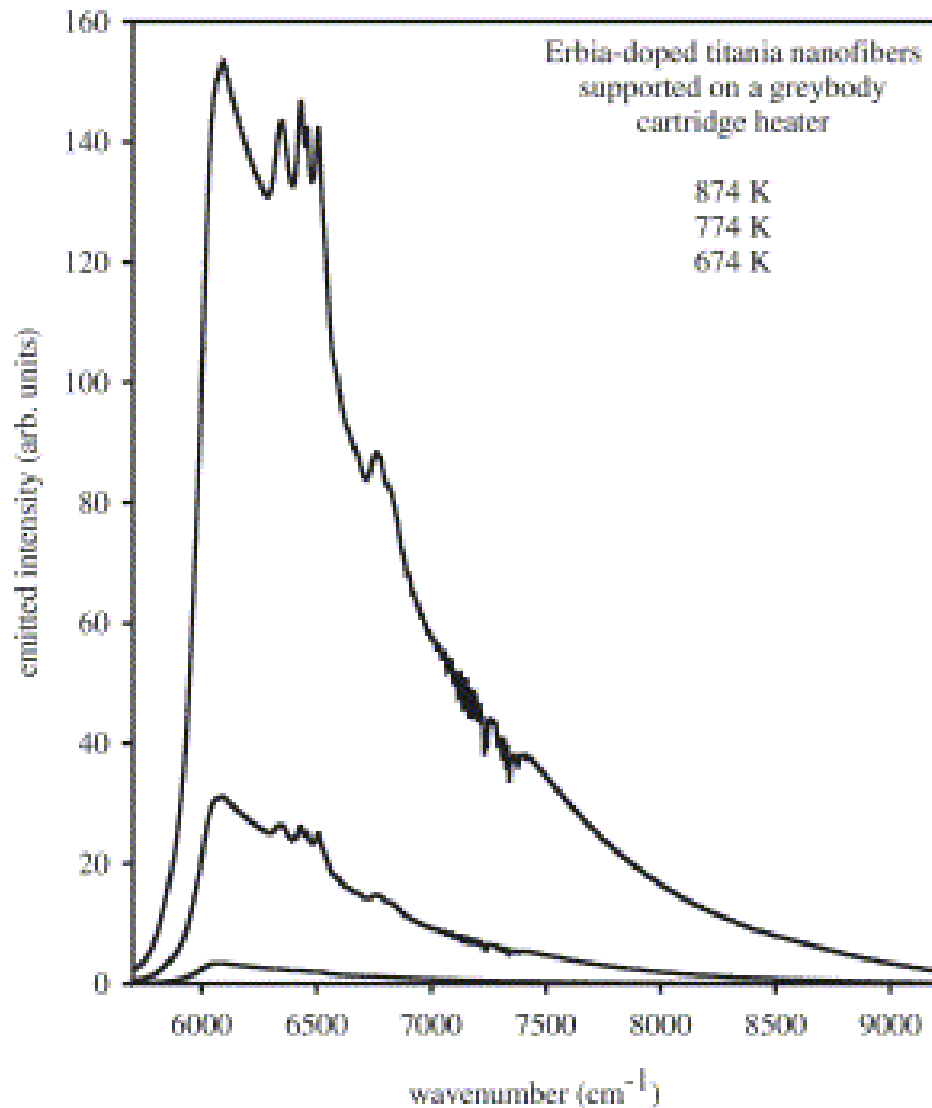
Figure 4. Spectra of Erbia doped titania nanofibers[8]

In contrast this absorption peak widens and weakens at a concentration level of 26% in a composite made from step sputtering [11]. Also another composite made by embedding the Ag particles in an amorphous Si matrix shows two absorption peaks at 350 nm and 700 nm with Ag concentration of 40% [10]. These differences can be attributed to the different particle sizes and different nano structures developed with different forming techniques. Different nano structures limit the mean free path of the conduction electrons, and the particle sizes affect the band structure. These two

16

effects modify the optical properties. The Sheng Ping effective medium theory [12], with the modification to account for the mean free path limitations, can be used to describe qualitatively the measured absorption spectra.
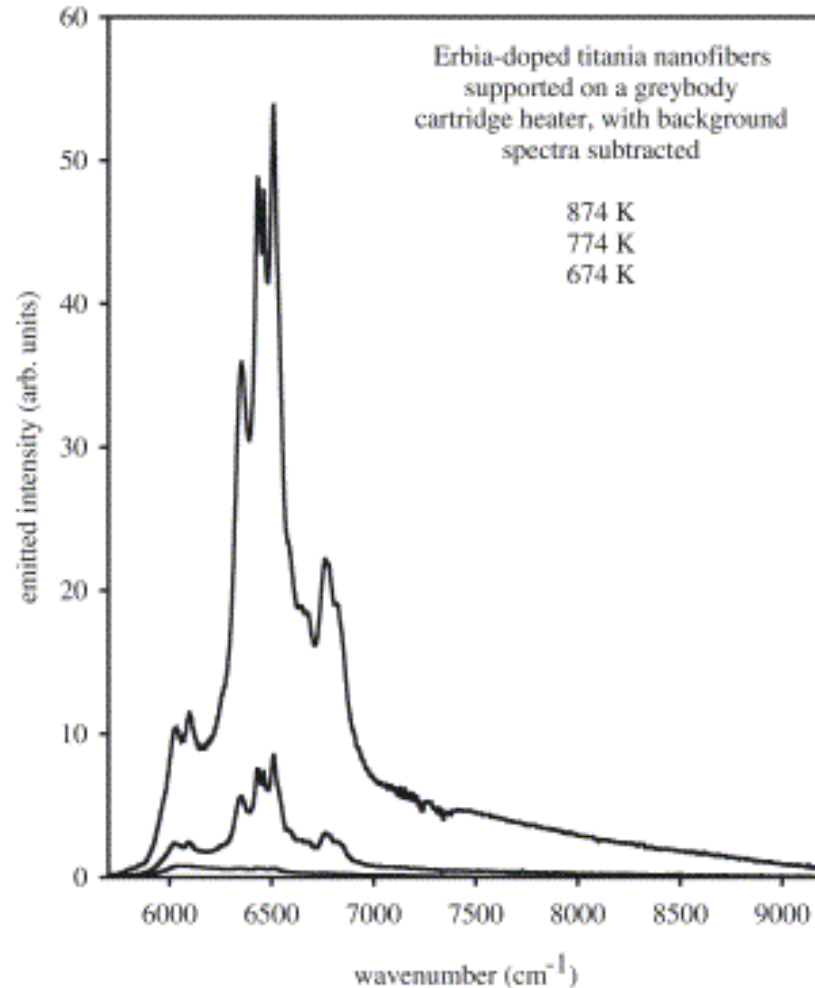
Figure 5. Spectra of Erbia doped titania nanofibers   (Background spectra subtracted)

These effective medium theories are not capable of describing the percolation phenomena, therefore they cannot be used to predict the outcome closer to the percolation threshold.

Even though there are a number of research projects conducted in these metal particles and insulator/ semiconductor compounds, all of them have targeted the same type of materials and forming techniques, therefore, not much significant knowledge has been added for the last 4-5 years. Even if some nano coatings could produce the desired optical properties, their applicability as a usable coating in practice is subject

17

to many other important considerations. These coatings may need to have good adhesion for some suitable substrates, thermal stability and durability for the desired application.
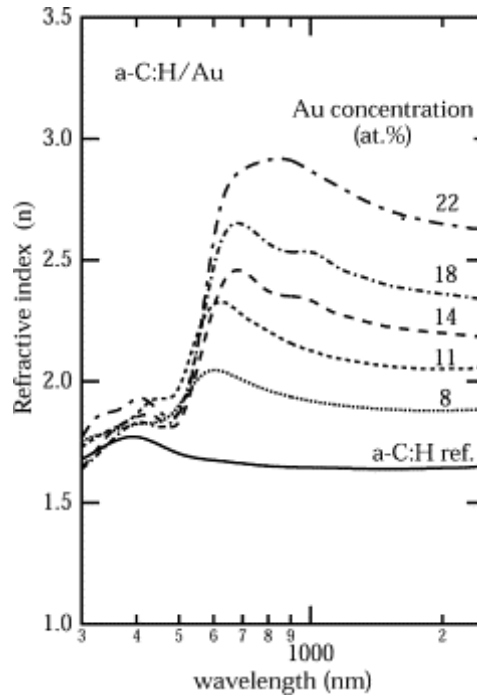
Figure 6. Refractive index variations of composite of Au and amorphous carbon [9]
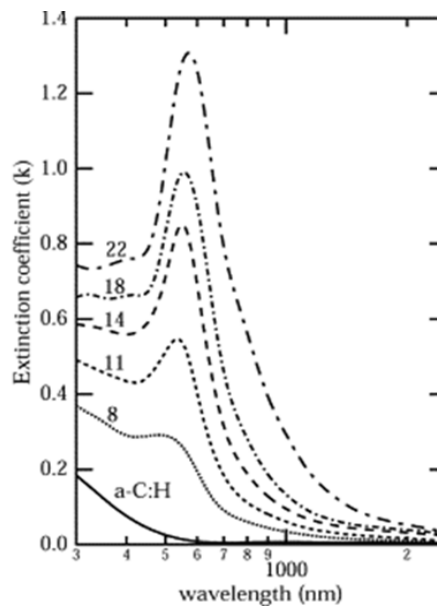
Figure 7. Extinction coefficient variations of composite of Au and amorphous carbon [9]

18

3.2 Development of Methodology to Evaluate the Thermal Emission

As explained in the section, 2.2, any potential definition of emitter efficiency should consider the intrinsic capabilities of the conversion mechanism in which these emitters are to be employed. In other words we have to consider the usability of the emitted radiation with respect to the conversion mechanism in order to evaluate their performances in an explicit manner. First we derived an expression for the "usability" of the radiation as explained below.

3.2.1 Derivation of an Expression " Usability" of the Radiation

To calculate the usability of incoming radiation consider a reversible (loss less), frequency dependent conversion mechanism in equilibrium with the environment at T_o as shown in figure 9. It is fed with a narrow band radiation source (figure 8) and produces an electric output. Let H_f be the total energy of radiation within the frequency range that matches the acceptable frequency range of the mechanism. Also let J_f be the amount of energy within this frequency range which is theoretically impossible to be converted by this mechanism (this may be due to any theoretical limitation of the system as illustrated in the photovoltaic example). The mechanism will deliver an output B_f and reject some heat q to the environment at T_o. If s is the entropy involved in $(H_f - J_f)$ and, as there is no entropy generation in the reversible mechanism, this entropy should be transferred to the environment via the rejected heat q and via the radiation emission from the conversion device surface (receiving surface) within the acceptable frequency range (e_f). The radiation emission within other frequencies can be minimized to zero using an antireflection coating. Also we assume that the temperature of the converting mechanism remains at the equilibrium temperature T_0. This assumption is justified as narrow band emitters are targeted to provide radiation within the required frequency range and therefore the

19

radiation outside of this frequency range which could heat up the mechanism can be negligible.
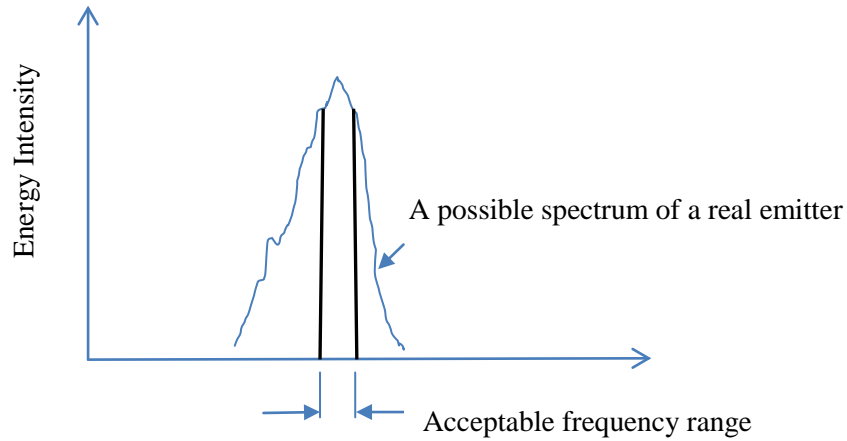
Figure 8. A possible spectrum of a real emitter that is designed to emit within acceptable frequency range.
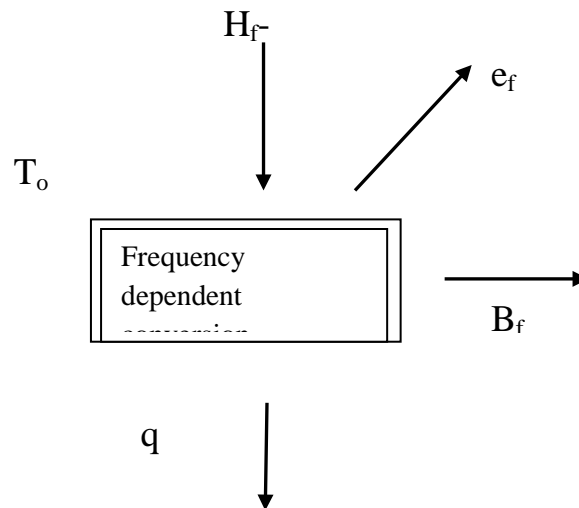
Figure 9. Energy balance of a frequency dependent energy conversion mechanism

From the entropy balance we have

$$s = \frac{q}{T_o} + S_e$$

Therefore
$$q = T_o\,(s - s_e) \qquad (4)$$

Looking at the energy balance

$$H_f - J_f = q + B + e_f \qquad (5)$$

20

Combining 4 and 5 we obtain

$$B = H_f - J_f - T_o (s - s_e) - e_f \qquad (6)$$

where,

H$_f$ - Energy within acceptable frequency range.

J$_{f-}$ part of energy within this frequency range which is theoretically impossible to be converted by this mechanism

B$_{f-}$ energy output (here the electrical energy output)

q- Heat rejected to the environment at T_0

e$_f$ - radiation emission from conversion mechanism surface (receiving surface) within the acceptable frequency range

S$_e$ – entropy associated with e$_f$

If the temperature of the emitting surface is much higher than the ambient temperature (assumes the energy conversion mechanism is at ambient temperature) the e$_f$ and therefore the entropy S$_e$ can be neglected for engineering calculations. The radiation energies of two surfaces are qualitatively depicted in figure 10.
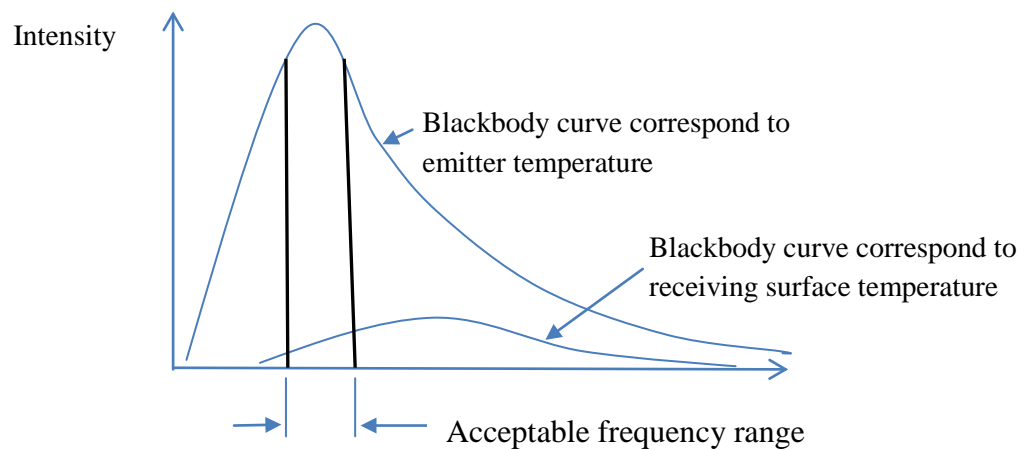
Figure 10. The radiation energies of the emitting and receiving surfaces

In the figure 9, B$_f$ is the energy output as electric power which is the usable energy within this radiation field. Another term for "usable energy" in thermodynamic terms is the "exergy". But here in our calculations we consider theoretical limitations by means of J$_f$, different from the standard limitations in conventional exergy calculations. Therefore the "usable energy" that we have calculated is different from

21

the conventional exergy definition. To distinguish this type of usable energy from conventional exergy, we call it "frexergy" because all the additional theoretical limitations we consider here are functions of frequency.

We define this "frexergy" as the part of exergy of spectral thermal radiation which adequately describes the potential to be converted to electricity by a given method of reversible, frequency dependent, conversion process at a given environment.

This frexergy is nothing but a part of the conventional exergy of a thermal wave field which we have to identify, based on the abilities of a given conversion process. Let's further illustrate the calculation of "frexergy" first by considering a rectenna and then, with the familiar photovoltaic cell as the frequency dependent conversion process.

3.2.1.1 Examples for Calculating "Frexergy"

3.2.1.1.1 Example 1 - Rectenna

A rectenna is a rectifying antenna, a special type of antenna that can be used to convert electromagnetic energy into DC electricity. This method has been successfully used to convert microwave radiation to electric power with high efficiency [13]. Recent research in this method is directed towards infrared and optical frequencies anticipating the conversion of solar power to electricity as an alternative method to conventional PV cells [14].

In a rectenna system, so far there is no known theoretical limitation regarding the conversion of thermal radiation within the acceptable range of the rectenna (unlike the band- gap limitations in photovoltaics). Therefore, J_f is zero and the frexergy equation is simplified to

$$B_f = H_f - T_o s \qquad (7)$$

22

Therefore, considering an arbitrary geometry of a radiation source, the frexergy can be calculated as:

$$B_f = \int_{v1}^{v2} \int_{\Phi1}^{\Phi2} \int_0^{2\pi} \int_A K(v, \Phi, \theta) \ cos\Phi sin\Phi \ dvd\Phi d\theta dA$$

$$- \int_{v1}^{v2} \int_{\Phi1}^{\Phi2} \int_0^{2\pi} \int_A T_0 S(v, \Phi, \theta) \ cos\Phi sin\Phi \ dvd\Phi d\theta dA \qquad (8)$$

where v_1-v_2 is the acceptable frequency range of the rectenna, K is the intensity of radiation as a function of frequency and direction and S is the corresponding entropy involved with K. A is the total area of the emitting surface, Φ is the inclination angle and θ is the azimuth angle.

3.2.1.1.2 Example 2 - Photovoltaic Cell

For solar cells only the radiation with frequencies above a cut-off frequency v_0 is usable for electric conversion, with the excess energy of the photons over the band gap energy rejected as heat. This limitation could be removed theoretically by means of an infinite number of junctions which together cover the whole spectrum up to infinity. But in practice this is not possible. Here for our illustration, consider a single junction PV cell. Considering an arbitrary geometry of a radiation source and after some simplification it can be shown that

$$H_f - J_f = \int_{v0}^{\infty} \int_{\Phi1}^{\Phi2} \int_0^{2\pi} \int_A \frac{v_o}{v} K(v, \Phi, \theta) \ cos\Phi sin\Phi \ dvd\Phi d\theta dA \qquad (9)$$

Please note the $\frac{v_o}{v}$ term accounts for the excess energy J_f being removed from the total energy H_f, because it is not usable by the PV device.

The entropy S within the energy H_f is

$$\int_{vo}^{\infty} \int_{\Phi1}^{\Phi2} \int_0^{2\pi} \int_A S(v, \Phi, \theta) \ cos\Phi sin\Phi \ dvd\Phi d\theta dA \qquad (10)$$

23

Therefore,

$$B_f = \int_{v0}^{\infty} \int_{\Phi_1}^{\Phi_2} \int_0^{2\pi} \int_A \frac{v_o}{v} K(v, \Phi, \theta) \, cos\Phi sin\Phi \, dv d\Phi d\theta dA -$$
$$\int_{vo}^{\infty} \int_{\Phi_1}^{\Phi_2} \int_0^{2\pi} \int_A T_0 S(v, \Phi, \theta) \, cos\Phi sin\Phi \, dv d\Phi d\theta dA \qquad (11)$$

All the parameters in this equation can be measured or can be calculated from measured values.

3.2.2 Use of the Frexergy Concept

3.2.2.1 The Criterion for Evaluation of Thermal Emitters

Now we are in a position to define the efficiency or effectiveness of thermal emitters using the frexergy concept defined earlier. Here we define an effectiveness based on frexergy to effectively evaluate the emitter performance. Thermal emitters are designed for specific type of applications such as targeting the frequency corresponding to the band gap of various types of solar cells (Cadmium telluride (CdTe), Copper indium gallium diselenide (CIGS), etc) or targeting the acceptable frequency range of different types of rectennas. The main purpose of this evaluation criterion is to distinguish the superiority of the wave fields produced by emitters for a given application.

We define a **quality factor** of an emitter as

$$\frac{frexergy \ of \ the \ emitting \ wave \ field}{Total \ energy \ of \ the \ emitting \ wave \ field} \qquad (12)$$

For the denominator we could use either the total energy input to the emitter or total energy of the emitting wave field. We selected the later due to the following reasons. As these emitters emit only the selected range of frequencies, often with a substantial energy input such as solar energy there is a possibility of accumulating the energy (as heat) within an emitter which increases its temperature. Therefore the practice is to use a buffer which can store this excess energy and utilize it at a later time when the original energy source is unavailable. For this reason it is complicated

24

to use the total energy input as the denominator. Also if we use total energy input, the energy losses from the other surfaces of the emitter device and the reflected radiation from the converting devise would have to be taken into account. Although these energies could determine the surface temperature of the emitter, and, therefore, the overall long-term efficiency, they have a minimum effect on the instantaneous efficiency, which is what matters most in electrical conversion.

Once we have decided to use the total energy of the emitting field as the denominator, we could use either the total energy of the emitting field or the total exergy of the emitting field. Using the total energy rather than exergy is more appropriate here as we describe below.

Consider an ideal selective emitter which can emit radiation exactly within the desired frequency range and zero emittance outside this range. If we use equation (6) to calculate frexergy, and use exergy of the wave field as the denominator then this emitter will have a quality factor of unity irrespective of the degree of coherence of the wave field. The degree of coherence is a significant factor which influences the entropy of the emitted field. Therefore it is required somehow to represent the degree of coherence or the influence of the degree of coherence (thereby the effect of entropy) in the quality factor to describe the wave fields with a higher degree of coherence. If we use the energy of the wave field as the denominator and again use equation (6) to assess the same ideal selective emitter, we get

$$\text{Quality factor} = \frac{H_f - T_o s}{H_f} = 1 - \frac{T_o s}{H_f} \tag{13}$$

As we can see in this expression, the quality factor approaches unity as the entropy approaches zero. Since a wave field with a higher degree of coherence has a lower amount of entropy the above expression gives higher values for the wave fields

with higher degree of coherence. Therefore we could justify the "quality" or high coherence by defining the quality factor as given in Eq. (12).

Although we could contrast the "usability" or "aptness" of different wave fields using a quality factor, it doesn't provide information about the spectral emisivities of the emitting surface. A high emissivity within the frequency range of interest is important for a higher power output from the conversion technique. Therefore we include a term called "effective emissivity" which is the mean emissivity of the surface within the considered frequency range and it is given by

$$\frac{\int_{v_1}^{v_2} k(v)dv}{\int_{v_1}^{v_2} k_b(v)dv} \tag{14}$$

where, K is the intensity of the radiation from the emitter and k_b is the blackbody intensity at the corresponding emitter temperature and $v_1 - v_2$ is the frequency range of interest. Then we can define the effectiveness of the emitter or emitting wave field as

$$\text{Effectiveness = effective emissivity * quality factor} \tag{15}$$

We choose to call it "**effectiveness**" of the emitter rather than efficiency because conventionally the efficiency is defined as the ratio of input to output, which is different from the ratio we have used here.

3.2.2.2 The Efficiency of Frequency Dependent Energy Conversion Methods

Conventionally, the exergy electric efficiency($\eta_{B,el}$) is defined as

$$\eta_{B,el} = \frac{E}{b} \tag{16}$$

where E- electrical output, b- exergy of the incoming wave field.

For conventional solar photovoltaic devices the incoming exergy b, is either the exergy of the solar radiation or the exergy of the concentrated solar radiation. If we can assume standardized values for the exergy of solar radiation and concentrated

solar radiation (depending on the concentration ratio) we will obtain fairly constant values for the electrical efficiency of any considered devise. But if we use a spectrally selective device for the incoming radiation, the situation becomes quite complicated. These spectrally selective devices can emit radiation with various spectral profiles and with different degrees of coherence. Therefore, there exists a huge range of values for exergy and hence for the efficiency. In other words the exergetic efficiency of the conversion device will depend on the types of emitter used. We can overcome this complication by defining the efficiency using the "frexergy" concept.

The exergy efficiency of the radiation conversion process can be defined effectively using frexergy as follows,

$$\text{Efficiency} = \frac{\text{electrical output}}{frexergy\ of\ the\ incident\ wave\ field} \tag{17}$$

By defining the efficiency this way we can evaluate the true intrinsic irreversibilities in the devise. Also it is to be noted that

Efficiency (frexergy) * quality factor =

$$\frac{\text{electrical output}}{frexergy\ of\ the\ incident\ wave\ field} * \frac{frexergy\ of\ the\ emitting\ wave\ field}{\text{Total energy }of\ the\ emitting\ wave\ field}$$

$$= \frac{\text{electrical output}}{\text{Total energy }of\ emitting\ wave\ field} \tag{18}$$

= conventional electrical energy efficiency (of the solar cell)

3.3 Derivation of the Exergy of a Partially Coherent Thermal Radiation

First we will derive an expression for exergy of quasi-monochromatic radiation using statistical thermodynamics and show that it is identical with the expression derived by Candau [15] using classical thermodynamic concepts. The significance of this statistical thermodynamic method is that it is consistent with the statistical method that is used to find the entropy of principle waves by Gamo [16]

27

and also this method is simple and far more detailed than Candau's method. Therefore we believe that this method facilitates the understanding of the concept of exergy of a partially coherent radiation. The derivation is presented below.

3.3.1 Derivation of the Exergy of Arbitrary Radiation
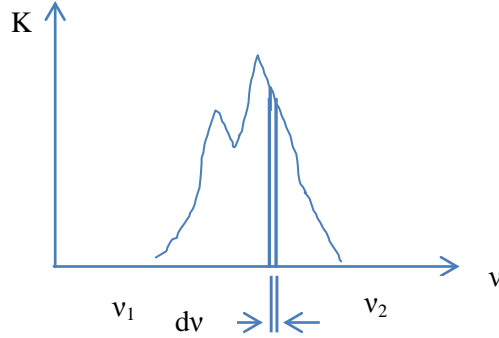
Figure 11. Spectrum of an arbitrary radiation

Consider a quasi-monochromatic beam in the frequency range [ν, $\nu+d\nu$] from an arbitrary spectrum as shown in figure 11. Let K_ν be the specific intensity of this beam at a frequency ν. Here the specific intensity can be defined as the energy emitted perpendicular to the area dA within a solid angle $d\Omega$ for the time interval dt and within the frequency range $d\nu$. Then the number of photons N, traversing through an area dA within a solid angle $d\Omega$ for the time interval dt by this beam of specific intensity K_ν is given by

$$Nh\nu = K_\nu d\nu dt dA d\Omega \tag{19}$$

where h is the Planck constant.

With reference to figure 12, state 1, consider this beam with N photons traveling in an environment at a temperature T_0. To find the exergy of this beam consider also a second state (state 2) that could be taken by these photons.

From the Gouy-Stodola law,

$$\text{Exergy loss } (\delta b) = T_0 * \text{ entropy growth } (\pi) \tag{20}$$

Therefore the exergy of a state = T_0 * maximum possible entropy growth.

28
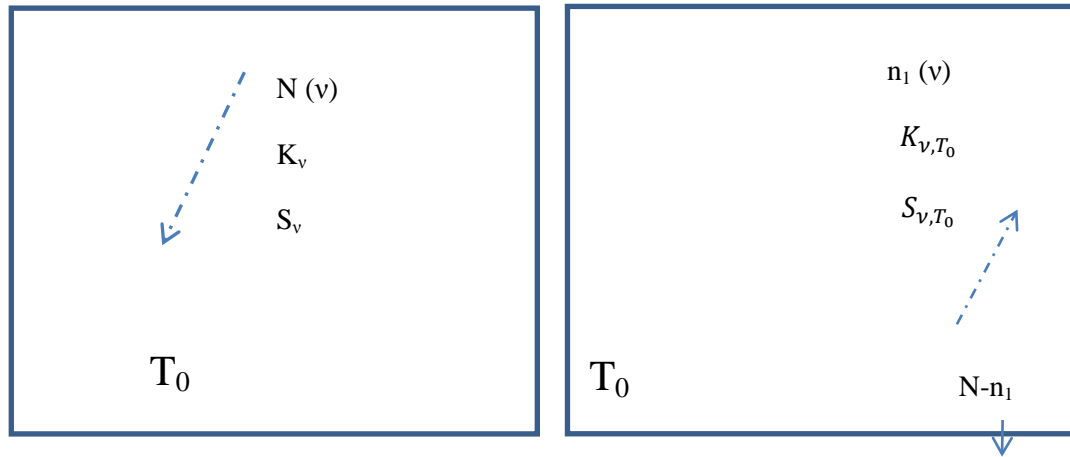
State 1   State 2

Figure 12. Two states of photons- State 1-Radiation beam with N photons, State 2-photons at the equilibrium state.

So to find the exergy of state 1 we need to find the maximum possible entropy growth from state 1 to state 2. According to statistical thermodynamics, the entropy of Bose-Einstein particles becomes a maximum for the well-known plank distribution. This means that N photons with a frequency v should be distributed as photons from a Blackbody at T_0 within the frequency range dv for maximum entropy, assuming the frequency v remains the same at state 2. But the number of photons within the frequency range dv from a Blackbody at T_0 is fixed by the plank distribution. Let this number of photons be n_1. Then for a general case where $N > n_1$ (the temperature corresponding to the considered quasi mono-chromatic beam is greater than the ambient) $N - n_1$ photons should be absorbed by the environment. i.e. the molecules present in the environment. If we also assume the ambient temperature remains T_0 at state 2, then the environments at state 1 and state 2 are identical and are at equilibrium. Therefore we don't have to consider the re-emission of absorbed ($N - n_1$) photons in our equations.

The entropy associated with absorbed photons at state 2

$$\frac{(N-n_1)h\nu}{T_0}$$

The entropy of the N photons at state 1 is

$$S_\nu$$

The entropy of n_1 photons at state 1 is

$$S_{\nu,T_0}$$

Therefore the entropy growth is

$$S_{\nu,T_0} + \frac{(N-n_1)h\nu}{T_0} - S_\nu$$

and the exergy of photons at state 1 is

$$\left[S_{\nu,T_0} + \frac{(N-n_1)h\nu}{T_0} - S_\nu \right] T_0$$

We can rearrange the above expression as

$$Nh\nu - n_1 h\nu - T_0 (S_\nu - S_{\nu,T_0})$$

so that

$$K_\nu - K_{\nu,T_0} - T_0 (S_\nu - S_{\nu,T_0}) \qquad (21)$$

equals the intensity of the considered quasi-monochromatic beam – intensity of

Blackbody radiation at T_0 and within the frequency range [ν, ν+dν] - T_0(entropy

associated with quasi-monochromatic beam with intensity K_ν- entropy of Blackbody

radiation at T_0 and within the frequency range [ν, ν+dν].

To find the total exergy of an arbitrary spectrum we can add all the spectral

exergies. Thus, total exergy =

$$B_T = \sum_{\nu_1}^{\nu_2} \{ K_\nu - K_{\nu,T_0} - T_0 (S_\nu - S_{\nu,T_0}) \} \, d\nu \qquad (22)$$

3.3.2 Calculation of the Intensity of Principle Waves

If the radiation beam that we considered in the previous section is partially

coherent we cannot use the corresponding blackbody entropy value for S_ν. To

30

calculate the entropy of a partially coherent field, first it is required to calculate the intensity of statistically independent waves called "principle waves" of the wave field. After calculating the entropies associated with these principle waves, the entropy of the whole field can be calculated by adding these entropies associated with the principle waves. In the next section we illustrate how to calculate the intensity of statistically independent "principle waves" of partially coherent thermal radiation using the method "matrix treatment of partial coherence" originally developed by Gamo (1964) [16].

If the wave amplitude $v(x)$ contains no spatial frequencies outside the range from –W to W, then it is completely determined by giving its sampled wave amplitudes at discrete points spaced $\frac{1}{2W}$ apart, in the following manner [16].

W- Spatial frequency limit (units m^{-1})

$$v(x) = \sum_{n=-\infty}^{+\infty} v\left(\frac{n}{2W}\right) u_n(2\pi Wx) \tag{23}$$

where

$$u_n(2\pi Wx) = \frac{\sin \pi(2Wx-n)}{\pi(2Wx-n)} \tag{24}$$
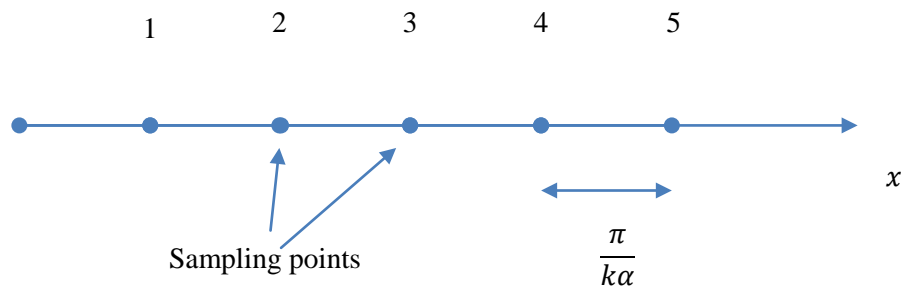

Figure 13. Sampling points that could be taken to measure the intensities.

If we consider a lens system with a numerical aperture $\alpha = n \sin \theta$ to measure the intensities, the spatial frequency limit is

$$W = \frac{k\alpha}{2\pi}$$

where k- is the wave number. Then the sampling interval $\frac{1}{2W} = \frac{\pi}{k\alpha} = \frac{\lambda}{2n\sin\theta}$.

For simplicity, let's consider a one dimensional radiating sample as shown in the figure 13. We can calculate the mutual intensities J_{12} at sampling points by using the apparatus shown in figure 14 and the procedure described below. Then we can create the intensity matrix in which an element A_{nm} of the intensity matrix can be represented as $J\left(\frac{m\pi}{k\alpha}, \frac{n\pi}{k\alpha}\right)$ which is the mutual intensity of the points m and n, with $A_{nm} = A_{mn}$

Then the principle intensities (x_j) are given by the eigenvalues of this intensity matrix. Also, the entropy remains unchanged by non-dissipative passive optical transmission such as shown in figure 14. Once the principle intensities are calculated the entropies associated with these intensities can be calculated using the methodology given in Appendix 2.
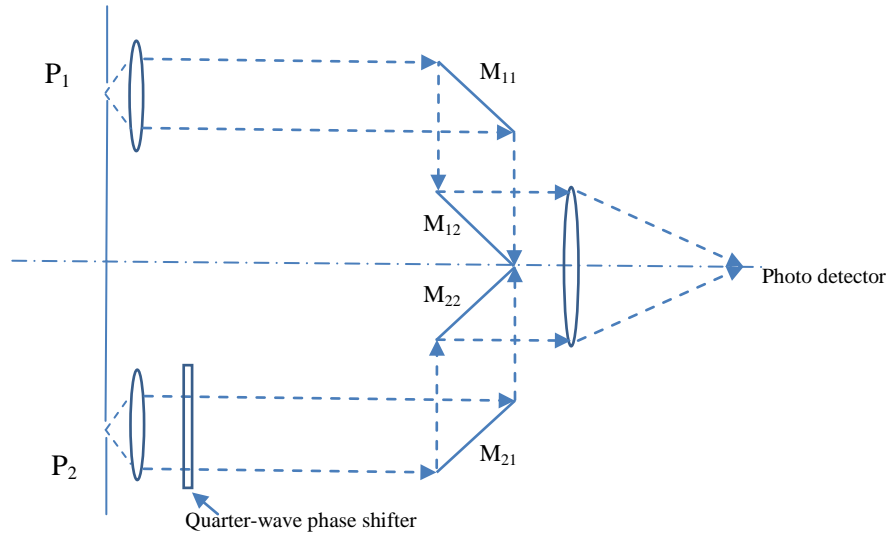

Figure 14. Measurement of mutual intensity using two point method [17]

The pinhole at p_2 is first closed and the intensity of the beam from p_1 is measured by a photo detector. The photo detector will then show a reading (I_1) proportional to the intensity at p_1. Therefore,

$$I_1 = b\, J_{11} \tag{25}$$

where, b is the proportionality constant.

By closing the pinhole at the p_1 intensity of the beam, from the p_2 beam one can measure

$$I_2 = b J_{22} \tag{26}$$

By opening both pinholes, the intensity of the superposed beam (I_3) can be found.

$$I_3 = b\, \{J_{11} + J_{22} + 2\,\mathrm{Re}\,(J_{12})\} \tag{27}$$

where Re (J_{12}) is the real part of the mutual intensity J_{12}.

After applying a quarter-wave phase-shift to one of the beams the intensity of the superposed beam (I_4) can be found again.

$$I_4 = b\, \{J_{11} + J_{22} + 2\,\mathrm{Im}\,(J_{12})\} \tag{28}$$

where Im (J_{12}) is the imaginary part of the mutual intensity J_{12}. Using equations (25), (26), (27) and (28) J_{12} can be calculated.

4. DESIGN AND FABRICATION OF A SURFACE PLASMON EMITTER

4.1 Surface Plasmons

Because of the interaction or "coupling" with the free electrons at the interface of a conductor (usually a metal) the electromagnetic waves are "trapped" on the surface creating surface plasmon waves. Due to this interaction of the light waves, electrons oscillate collectively in resonance with the frequency of the light wave giving rise to some unique properties. These surface waves propagate along the interface and decay exponentially in the perpendicular direction with increasing distance from the surface.

Because of the unique properties of the surface plasmons (SPs) and the electromagnetic energy density associated with them, they are of interest to a wide range of scientists, from physicists to biologists. Thermal emission of a material is controlled by the surface morphology and the excitation of surface waves. The thermal emission in the vicinity of a flat metal surface is quasi-monochromatic in a distance that is of the order of a wavelength, due to the excitation of surface plasmons. The interest is to couple these surface waves with propagating waves to have a quasi-monochoromatic radiation field in the far field. The most pragmatic way of doing this is to establish grating on the surface. The grating will then diffract the surface waves. Recent advances in nanotechnology that allow metals to be structured and characterized on the nanometer scale have rekindled interest in SPs. SPs are now being widely explored in various fields such as optics, magneto-optic data storage, microscopy and solar cells. The angle of propagation of the diffracted light can be changed by controlling the period of the grating. From Kirchhoff's law, absorptivity is

34

equal to emissivity for a given frequency. So by designing the surface with total absorption for a frequency which lies within a region where Planck's function takes large values we can create an efficient source of light. As the Planck'sfunction depends on the temperature of the source the optimum frequency too depends on the temperature.

4.2 Basics of Surface Plasmons (SP)

The SP dispersion relation for a flat air /material interface

$$k_{sp} = \frac{\omega}{c} \sqrt{\frac{\varepsilon(\omega)}{\varepsilon(\omega)+1}} \quad , \tag{29}$$

where, k_{sp} is the wave vector parallel to the interface, $\varepsilon(\omega)$ is the real part of the frequency dependent dielectric function of the material and $\omega = 2\pi f/\lambda$ is the angular frequency. Such SP waves exist for materials having the real part of $\varepsilon(\omega) < -1$ [18]. Only the metals and polar materials fulfill this requirement. By solving Maxwell equations for the dielectric/ metal interface it can be shown that only transverse magnetic (TM) waves could be coupled [19]. The equation for coupling the SP with incoming waves on a surface with texture periodicity or lattice constant **a** is

$$k_{SP} = k_0 \sin\theta \pm n \frac{2\pi}{a} u_x \tag{30}$$

where $\mathbf{k}_o = \omega/c$ is the incident wave vector, θ is the angle of incidence and u_x is the unit vector on the surface.With the $|\varepsilon(\omega)| \gg 1$ for a metal and by solving equations (29) and (30), for emission perpendicular to the surface, i.e. $\theta = 0$, it can be shown that for the coupling of SP with a wavelength **λ,** the periodicity **a** $\approx\lambda$ for metals.

4.3 Requirements of an Emitter for an Energy Application

For energy applications in general, it is desirable to assume a spectral profile with a narrow frequency range and an emissivity close to unity in the selected frequency range.

Therefore, the parameters of the grooves **b, d** and **h** have to be optimized for a narrower bandwidth and for a higher intensity (Fig. 15). If **b > λ/2, the** *wave propagating modes* are transmited through the holes leading to a much broader reflection minimum, therefore causing a broader emission maximum, which is not desirable. **b << λ/2** leads to a narrow but weaker absorption peak resulting in a considerably lower emission than the corresponding blackbody value. Also the higher depths **h** produce a wide spread in the emission peak.
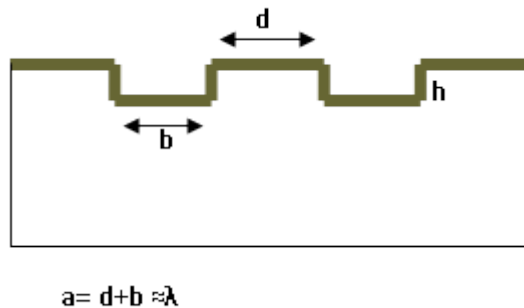

$a= d+b \approx \lambda$

Figure 15. A cross section of a plasmonic emitter

4.4 Optimization Approach of the Dimensions of the Emitter

One approach to optimize the dimensions of the grooves is by performing a numerical simulation. The Rayleigh hypothesis is used commonly for modeling the space at the metal (grating) / air interface, but many have argued the validity of this hypothesis especially at higher depths. Even though there are some other methodologies, such as the Chandrasekhar method, no methodology is capable of handling a complex structure with good accuracy. Although for a simple analytical surface profile, such as a sinusoidal profile, the simulation and experimental results agree with reasonable accuracy, for profiles with triangular or square type cross

36

sections there is a considerable discrepancy between theory and experiment. In practice no profile can be made perfectly smooth and any secondary roughness, other than the grating pattern, produces second harmonics with waves causing deviations from the computed values. The roughness, the consistency and the accuracy of the profile are functions of the fabrication process, quality control, etc., and it is hard to quantify these factors in the simulation program. As our requirement is to build an efficient pragmatic source, to test and demonstrate our evaluation criterion, the experimental approach is considered as the most appropriate method. With the constraints regarding the width and depth, and with knowledge of the outcome from published results, certain initial values were assumed for the groove dimensions. To optimize these parameters by an **experimental method** for a wavelength (λ), initial values for **a, b, d** & **h** were selected as follows:**a ≈λ, a = b+d,** filling factor **q= d/a ≈** 0.54 [20] and 0.5 λ >h> 0.1 λ [8]

4.5 Material Selection for the Emitting Layer

For a Silicon substrate, it is required to select a proper metal for depositing the emitter structure to activate the surface plasmons. As described earlier only the TM waves are enhanced and coupled by the surface plasmons. Thus, it is necessary to suppress the unwanted transverse electric (TE) emission. We can minimize the transverse electric (TE) emission by selecting a metal with low emissivity. Most metals exhibit very low emissivity less than 0.1 at infrared frequencies. But some metals like Aluminum forms an oxide layer which increase the emissivity considerably and this should be avoided. Therefore a common and cheap metal Nickel, which reacts slowly with the environment, is selected as the depositing metal.

37

4.6 Periodicity Calculations for Nickel Deposited Grooves

The dielectric function of a material (ε) can be written as

$$\varepsilon = \varepsilon_1 \pm i\varepsilon_2 = (n \pm ik)^2 \tag{31}$$

where,

$\varepsilon_{1=} n^2 - k^2$

$\varepsilon_{2=} 2nk$

Also, n= frequency dependent refractive index, k= extinction coefficient.

The peak of the emission profile is to be at 10 µm, Therefore Nickel at

9.53µm, n=6.44 and k= 35.3 [21] (from the data catalog)

$$\varepsilon_{1=} (6.44)^2 - (35.3)^2 = \text{-1204.6 F/m}$$

By inserting this value in equation (29) we obtain

$$k_{sp} = \frac{\omega}{c}\sqrt{0.9996}$$

Using equation (2)

$$\underline{a = 1.0004 \, \lambda}$$

4.7 Skin Depth (δ_o) Calculation for Nickel at 10 µm

$$\delta_O = \frac{\lambda}{4\pi k} \tag{32}$$

where Nickel at 9.537 µm

$$\frac{\lambda}{4\pi k} = \frac{9.5 \times 10^{-6}}{4\pi \times 35.3} = 21.4 \text{nm}.$$

Samples with varying important parameters were fabricated on a silicon wafer using typical lithographic techniques. The process flow of the fabrication is listed below. An optically thick (thickness greater than the skin depth) thin film of the metal (nickel), is required for the plasmon enhanced emission. So with a safety factor approximately equal to 5, a metal layer with thickness of 100 nm ($\approx$ 21.4x5) was deposited on the surfaces.

38

4.8 Process Flow Steps for Grating Fabrication

1- 4" <100> Silicon wafer

2- Clean wafer

3- Deposit ~200 nm SiO2 (Mask layer for the photoresist)

4- Spin photoresist on the wafer

5- Expose for the desired time

6- Develop for the desired time

7- Dry

8- RIE Etch the SiO2 completely (Use the PR as a mask)

9- Strip PR and clean

10- DRIE (desired depth- 1-2 micron)

11- RIE to remove the remaining SiO2
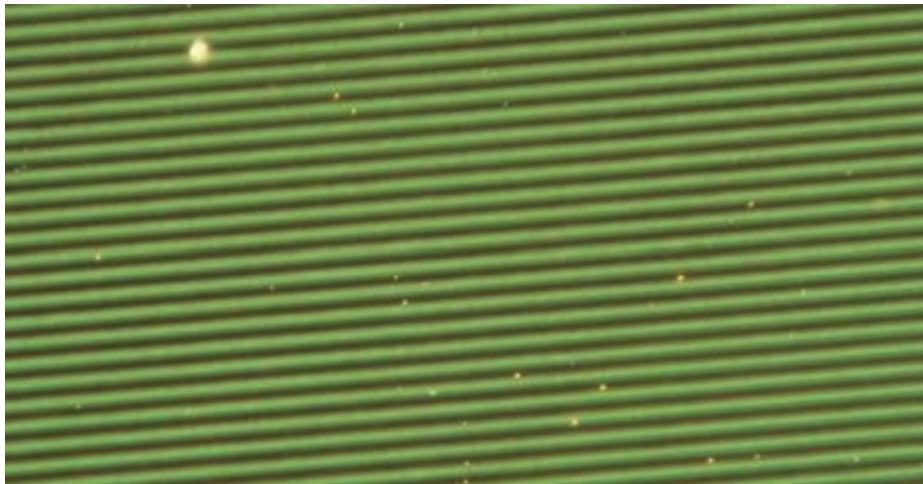
12- Deposit METAL (Nickel 100 nm) for testing

Figure 16. Appearance of the final product, the surface plasmon emitter

5. FUTURE DIRECTIONS FOR THE DEVELOPMENT OF THE SELECTIVE EMITTERS

5.1 Thermal Management of the Emitting Structure

The biggest challenge to a higher efficiency comes from two heat transfer mechanisms, conduction and convection. Published data showed that at high temperatures, several hundred degrees Kelvin, most of the energy of emitters is being dissipated through conduction and convection than the desirable radiation mode [22]. Therefore, it is required to reduce the conduction and convection to the atmosphere by suitable techniques, such as vacuum packaging. Also, a higher thermal conductivity is required to transfer the incoming energy effectively to the emitting surface. Similarly it is desirable to have a higher energy capacity within the emitter structure to avoid high temperature fluctuations. It may be appropriate to use a cheaper material except at the emitting surface to increase the mass and therefore the heat capacity. However, additional layers of materials reduce conductance especially when the layer thicknesses are very small (order of 100nm). Proximity of interfaces and micro-volumes of heat dissipation influences the thermal transport in an abrupt way causing problems of thermal management. There are two types of heat carriers in solids: electrons and phonons. A phonon is a quantum of crystal vibrational energy and is analogous to photon. Planck-like distribution of photons is radiated from the surfaces of solid and within the solid there is a distribution of Planck-like phonons. Phonons have two fundamental lengths: wavelength and mean free path. At room temperature, the dominant heat-carrying phonons typically have wavelengths of 1-3 nm and mean free paths of 10-100 nm.

When the material sizes are comparable with the phonon mean free path, phenomena such as phonon interference may occur and the macroscopic approach to conductance, i.e. Fourier's law is no longer valid. Therefore, we cannot select materials based on their listed macroscopic conductivity values, as at this small scale these values have little meaning. The thermal transport analysis should be carried out for the whole emitting structure comprising of all the essential layers. Therefore, selection of proper materials by considering an enhanced thermal transport is difficult as it is required to consider a number of combinations of materials to find the optimum. Although the thermal conductivities of nanosclae films of about 100nm were measured the direct measurement tools are not accurate enough to measure the films less than 100nm. Although the practicability of the scanning thermal microscope for a quantitative measurement of the local heat conductivity at material surfaces are good enough [23, 24], Molecular dynamics simulations [25] the Boltzmann transport equation [26] and the lattice Boltzmann method (LBM) [27] might be better options to analyze the emitter structure over the experimental methods. They were used to analyze the phonon transport in nanometer films as effective tools for calculations and understanding of thermal conductance and phonon scattering when direct measurements are difficult to perform.

5.2 Performance and Cost Optimized Thermal Emitters

From the published literature it is found that 1) Hexagonal hole arrays, 2) rectangular periodic cavities and 3) Grooves, are the favorable designs for plasmonic emitters considering both simplicity and performance. But there is no information to compare these 3 designs. So it is recommended to fabricate these 3 types of emitters for the same wave length using the same material and with the same tolerances, surface finish, etc. and measure their performances. For simplicity we could take the

41

quality factor of the emitting profile as the performance index. The quality factor =

peak wavelength/ FWHM, where FWHM is full width at half maximum.
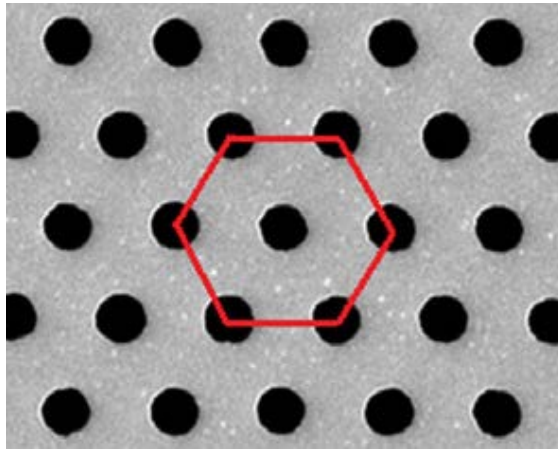

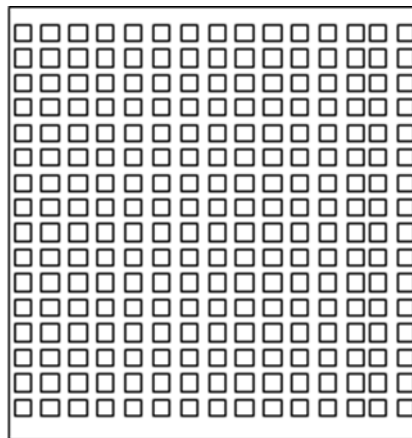Figure 17. Hexagonal hole arrays [28]

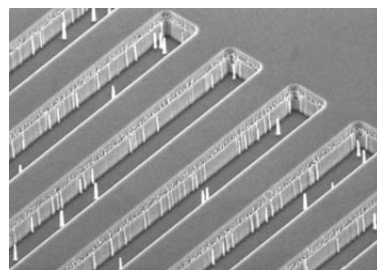Figure 18. Rectangular periodic cavities

Figure 19. Grooves [20]

If we select a frequency within infrared range the results could be generalized to whole infrared range as the material properties of interest do not change much within the frequency band. However, if we want to compare the performance in the optical range we need to measure their performances using a frequency from optical range. If we use a metal as the material we could generalize the results qualitatively to other metals as the material properties of interest for metals do not vary much in a specific frequency range. If we want to compare the performances of these 3 designs with another material such as a conductive polymer we need to do whole set of experiments again.

Energy and economy are highly interrelated; therefore any component that is to be used in energy related applications should be made economically. Surface plasmon emitters, currently at the research level have shown promising performances, but their manufacturing costs are high as they are manufactured mainly using expensive MEMS technologies. So to reduce their costs economical industrial methods for manufacturing these devices must be found. Manufacturing costs are expected to reduce with time as micro manufacturing technologies are improving rapidly. So it is expected that the fabrication costs of these devices will be low enough to use them in energy applications.

Manufacturing performance specifications of interest for the emitters include minimum feature size, feature tolerances, feature location accuracy, etc. In general the technologies with high precision (high accuracy, good surface finish) are expensive. Therefore if we use a technology with higher precision than required we are spending more and if we employ a technology with a lower precision we will not be able to meet the required performance. So to find a proper technology to manufacture, the knowledge of *acceptable* feature tolerances, feature location accuracy, surface finish,

43

etc of these emitters is required. To determine these acceptable parameters we have to know how the emitter performance varies with these parameters. But this critical information is not yet known. Once a proper design is selected experiments could be conducted to study the variation of performance index with the feature size.

6. SUMMARY

This dissertation has presented an improved understanding of selective emitters for energy applications. We have presented a criterion for the formation of spectrally selective paints for energy applications such as solar thermal conversion and radiative cooling followed by a compilation of the optical properties of pigments, resins, and solvents which can be used to formulate paints with desired selective emittance. Also we discussed the possible future research opportunities to optimize these coatings and paints to achieve narrow spectral selectivity that is needed for Thermophotovoltaic and Rectenna applications. In addition we identified the possible areas that should be addressed to improve the performances of advanced emission control mechanisms that can be used in energy applications.

In the past, exergy of thermal radiation was defined only for theoretical interest, mainly to find the upper limit of solar energy conversion and was widely considered as a concept with little practical significance. Using statistical thermodynamics we derived an expression for the exergy of arbitrary thermal radiation and we described much overlooked relationship between entropy and degree of coherence for the evaluation of thermal emitters for energy applications. Based on this research we developed a practical and useful meaning of thermal radiation exergy. We developed rigorous evaluation criteria for thermal emitters which can be used to find the appropriateness of these emitters for any radiation conversion technique. A surface plasmonic emitter was fabricated using MEMS techniques to demonstrate the evaluation criteria.

REFERENCES

[1] El-Kady, I. G. B. Farfan, R. Rammohan, M. M. Reda Taha, Photonic crystal high-efficiency multispectral thermal emitters, Applied Physics Letters 93 (2008) 15350.

[2] Farfan G.B., R. Rammohan , M.F. Su , I. El-Kady , M.M. Reda Taha, Prediction of photonic crystal emitter efficiency using an optimized fuzzy learning approach, Photonics and Nanostructures – Fundamentals and Applications. 6 (2008) 154–166.

[3] Orel ZC, Gunde MK. Spectrally selective paint coatings: preparation and characterization. Solar Energy Materials and Solar Cells 2001;68:337–53.

[4] Chalmers JM. Infrared spectroscopy in the analysis, characterization, and testing of coatings. JCT Journal of Coatings Technology 2005.

[5] Brady RF, Wake LV. Principles and formulations for organic coatings with tailored infrared properties. Progress in Organic coatings 1992; 20:1–25.

[6] Thiele ES, French RH. Light-scattering properties of representative, morphological rutile titania particles studied using a finite-element method. Theory and Modeling of Glasses and Ceramics 1998;79:469–79.

[7] Gardner/Sward. Paint testing manual. 13th edition ASTM International; 1972.

[8] Tomer V, Teye-Mensah R, Tokash JC. Selective emitters for thermophotovoltaics: erbia-modified electrospun titania nanofibers. Solar Energy Materials and Solar Cells 2005;85:477–88.

[9] Oelhafen P, Schuler A. Nanostructured materials for solar energy conversion. Solar Energy 2005;79:110–21.

[10] Niu F, Cantor B, Dobson PJ. Microstructure and optical properties of Si–Ag nancomposites films prepared by co-sputtering. Thin Solid Films 1998;320:184–91.

[11] Wang Q, Yang B, Tian D, Xiong G, Zhou Z. The optical properties of Ag–Si nanocomposites films prepared by sputtering. Surface and Coatings Technology 2000;131:404–7.

[12] Sheng P. Theory for the dielectric function of granular composite media. Phys Rev Lett 1980; 45:60.

[13] Brown W. C., The history of wireless power transmission, Solar Energy. 56 (1996) 3-21.

[14] Goswami D. Y., S. Vijayaraghavan, S. Lu, G. Tamm, New and emerging developments in solar energy, Solar Energy 76 (2004) 33-43.

[15] Candau Y. On the exergy of radiation. Sol Energ 2003;75:241e7.

[16] Gamo H. Thermodynamic entropy of partially coherent light beams. Journal of the physical Society of Japan 1964; 19(10): 1955-61

[17] Born M, Wolf E. Principles of optics. Cambridge press: 1999. (Chapter 10)

[18] Raether, H. Surface Plasmons (ed. Hohler, G.) (Springer, Berlin, 1988).

[19] Ye Y.-H., J.-Y. Zhang, Appl. Phys. Lett. 84 (2004) 2977.

[20] DAHAN, N. et al. Extraordinary Coherent Thermal Emission From SiC Due to Coupled Resonant Cavities. Journal of heat transfer. 130 (2008) 112401-1

[21] Palik E.D. Handbook of Optical Constants of Solids.

[22] Lezec H. J., A. Degiron,1 E. Devaux, R. A. Linke,L. Martin-Moreno, F. J. Garcia-Vidal, T. W. Ebbesen; Beaming Light from a subwavelength Aperture; SCIENCE, 297, 820-822; (2002)

[23] Fischer H.; Quantitative determination of heat conductivities by scanning thermal microscopy; Thermochimica Acta 425 (2005) 69–74

[24] Yu-Ching Yang, et al; Modeling of thermal conductance during microthermal machining with scanning thermal microscope using an inverse methodology Physics Letters A; (2007)

[25] Wang Zenghui, et al; Lattice dynamics analysis of thermal conductivity; Applied Thermal Engineering 26 (2006) 2063–2066

[26] Flores Renteria A., et al; Effect of morphology on thermal conductivity Surface & Coatings Technology 201 (2006) 2611–2620

[27] Hongwei Liu, et al; Monte Carlo simulations of gas flow and heat transfer in vacuum packaged MEMS devices; Applied Thermal Engineering 27 (2007) 323–329

[28] Ziambaras E., et al; Thermal transport in SiC nanostructures Materials Science and Engineering C 25 (2005) 635 – 640

[29] Aleksander S. Radiant properties of materials: tables of radiant values for black body and real materials. New York: Elsevier; 1986.

[30] Lewis P. Pigment handbook. 2nd ed. John Willey & Sons; 1988.

[31] An infrared spectroscopy atlas for the coatings industry. Federation of Societies for Coatings Technology 1980.

[32] Touloukian YS. Thermal radiative properties: coatings. New York: IFI; 1972

[33] Mandel L, Wolf E. Optical coherence and quantum optics. Cambridge press: 1995.

[34] Wijewardane S., Goswami Y., Exergy of Partial Coherent Thermal Radiation, Energy (42) 2012 497-502

[35] Wijewardane S., Goswami Y.,. A review on surface control of thermal radiation by paints and coatings for   new energy applications; Renewable and Sustainable Energy Reviews (16) 2012 1873-1883

APPENDICES

Appendix 1 Absorption Properties of Selected Materials

All most all the energy related applications of selective paints and coatings desire a high emittance at a particular frequency or within a particular frequency range. According to Kirchhoff's Law emissivity equals the absorptivity at a given frequency. Therefore we compiled the pigments (Table 1A) resins (Table 2A) and solvents (Table 3A) with high absorption peak or high absorption frequency range that can be used to formulate paints with desired selective emittance. Also we tabulated selected paints (Table 4A) and coatings (Table 5A) which have high absorption at a particular frequency or within a frequency range.

Table A1. Pigments with high absorption peak (s) or range. [29, 30, 31]

Pigments	Peak absorptance Wave length (s) (μm)
Aluminum Silicates	7.7
Calcium Carbonate	6.7
Calcium Phosphosilicate	9.5
Calcium Borosilicate	9.8
Sodium Silicates	10
Sodium Sulfate	8.8
Calcite	7
Cobalt Aluminate	15.4
Fe2O3	17.5, 25
Zinc Chromate	2.9, 11.1
Asbestos	10.4
Cu, Cr (Black)	16.4, 19.2
Nichem	2.9, 6.2, 11.8

Table A2. Resins with high absorption peak(s) [31]

Resin	Peak absorptance Wave length (s) (μm)
Poly (acrylamide)	6
polyacrylic Acid	5.8
Methyl Methacrylate (**Acryloid**)	5.8
Acrylic Copolymer	5.8
Acrylate Homopolymer	5.8
poly (Lauryl Methacrylate)	3.4
polymethacrylic	5.9
Alkyd	5.8
Cellulose Acetate Butyrate	5.7, 8.6
Cellulose Acetate	5.7, 8.1
Methyl Cellulose	9.3
Nitrocellulose	6, 7.8
Tetrafunctional Epoxy Resin	6.6
Epoxy Novolac	6.6, 8.1
Polyglycol Epoxy	9.1
Butyl Glycidyl Either Epoxy	3.3, 8.9
Epoxy Ester	3.4, 6.6
Amine based Epoxy resin	6.6
Hydanation epoxy resin	5.8
Brominated Bisphenol	3.4, 6.6, 8
Novolac Epoxy	3.4, 6.8, 8.2, 9.8
Bisphenol	6.6, 8
Hexamethoxymethyl Melamine	3.4, 6.4, 9.2
Methylated Melamine Formaldehyde	6.5
Methylol Melamine	6.5
Metal salt of Resin Acids	3.4, 6.3
Polymerized Resin	3.4, 5.8
Polyamide resin	3.4, 6
Isophthalate Polyester	5.8, 8
Polyester Polymers	5.8, 7.8
Polyethylene Glycol	3.4, 8.9
Methyl Vinyl Ether	5.6
Polyvinyl Ethers	3.3, 9.3
PolyGlycol	2.9, 3.5, 8.9
polyethylenimines	3.4, 8.7
Polyurethane Polymers	3.3, 4.5, 5.7, 8.2
Silicone	9.1
Dimethyl Polysiloxane	7.9, 9.5, 12.5
Sodium Methyl Siliconate	8.9
Methyl Phenyl Polysiloxane	7.9, 9.5, 12.5
Poly Vinyl Butyral	3.4, 8.8, 10
Poly Vinyl Alcohol	3.4, 8.8, 10
Polystyrene	14.3
Polyvinyl Acetate	5.7, 8.1
polypropylene	3.4

Table A3. Solvents with high absorptance peak(s) [31]

Solvent	Peak absorptance Wave length (s) (μm)
Benzyl Alcohol	3, 6.9, 9.1, 13.7
Butanol	3, 3.3, 7.4, 8.2, 10.9
Diacetone Alcohol	5.9
Ethanol	3, 3.3, 9.5
Isobutanol	3, 3.3, 9.5
Methanol	3, 9.5
Ethyl Acetate	5.7, 8
Ethyl Isobutyrate	5.7, 8
Methyl Amyl Acetate	3.3, 5.7, 8
Cyclohexane	3.4
N-Pentane	3.4
Benzene	3.3, 6.8, 14.5
Carbon Tetrachloride	12.8
Chloroform	8.2, 13.3
Perchloroethylene	11
Tetrachloroethane	8.3, 12.5, 13.3, 18.2
Trichlorobenzene	6.9, 9.2
Trichloroethane	9.3, 14.1
Dipentene	3.4, 6.9, 11.4
Turpentine	3.4
Tripolene	3.4
Acetone	5.8, 8.2
Pentoxone	3.3, 8.2, 7.4, 9.3
Propylene Carbonate	5.6, 8.4, 9.5

Table A4. Some selected paints with high absorptance peak(s) or range [32]

Paint	Peak absorptance Wave length (μm)	Absorptivity
Antimony trioxide in Potassium silicate binder	0.3	0.9
CaF2 in sodium silicate binder (exposed to ultraviolet Radiation)	0.3	0.8
Sodium aluminum silicate in sodium silicate binder (exposed to nuclear radiation)	0.4	0.9
TiO2 in silicone resin binder	0.4	0.9

Table A5. Some selected coatings with high absorptance peak(s) or range [32]

Coating	Peak absorptance Wave length (µm)	Absorptivity
50% Co, 50%W on sandblasted substrate, heated to 1000K	2	0.85
Al2O3 (0.4 mm thick) on roughned stainless steel substrate	9.5	0.98
BaO.TiO2 powder (0.127 mm thick) on Zr alloy substrate	11.5	0.98
B4C on Inconel sandblasted substarte heated to 1000K	5,10	0.99
Pyrolytic graphite, vapor deposited at 2400K	1.5	0.83
TiO2, (0.064 mm thick) on Niobium substrate	0.7	0.95
Zirconium Oxide on sandblasted Inconel substrate	12	0.95
ZrO2.SiO2 (0.1mm thick) on Nb, Zr alloy substrate	8	0.95
Anodized Al (2 µm thick) Sulfuric acid anodized	11	0.8
NiCrOx on stainless steel substrate	0.8	0.95
Si3N4 on Al substrate	10	0.95
Fe2O3 on Stainless steel substrate	0.8	0.98
Cr2O3 on Stainless steel substrate	0.8	0.85
CuO on Stainless steel substrate	0.8	0.95
PbS on silver substrate	0.8	0.95
	High absorptance Wave length range (µm)	**Absorptivity**
Calcium titanate (0.09 mm thick) on rough niobium substrate	2-13	0.9
85% Cr2O3, 10 % SiO2 on mild steel substrate	2-14	0.9
Fe2O3 (0.03 mm thick)	3-21	0.9
Iron Titanium, Aluminum Oxide (0.1 mm thick) on Nb, Zr alloy substrate	1.5-13	0.9
MgO.Al2O3, (0.13 mm thick) on Nb, Zr alloy substrate	6-12	0.9
KBr (7.5 µm thick) platinum substrate	104-108	0.98

Appendix 2 Entropy Calculation

Calculation of S_v, the entropy associated with quasi monochromatic light beam is presented below. The following discussion is based on the reference [33]. The entropy of a quasi-monochromatic light using Bose-Einstein formula is given by

$$S= kg\left\{\left(1+\frac{N}{g}\right)log\left(1+\frac{N}{g}\right)-\frac{N}{g}log\frac{N}{g}\right\}\tag{1}$$

g- Number of degrees of freedom of the wave field

N-Number of photons per principle wave

k- Boltzmann constant

The number g in phase space is given by

$$g=\frac{dxdydzdp_xdp_ydp_z}{h^3}\tag{2}$$

where dp_x is the magnitude of the momentum of a photon in x-direction, and h is the Planck constant. Inserting $dA=dxdy$, $dz=cdt$ and $p=\frac{hv}{c}$ in equation (2), we get

$$g=\frac{v^2}{c^2}dvdtdAd\Omega\tag{3}$$

$d\Omega-$ element of solid angle around the direction of propagtion from a surface element dA

By considering the sample interval,

$$\frac{\pi}{k\alpha}=\frac{\pi}{kn\theta}$$

$$dA=(\frac{\pi}{kn\theta})^2 \text{ and } d\Omega=\theta^2$$

Therefore

$$n^2dAd\Omega=\frac{\bar{\lambda}^2}{4}\tag{4}$$

where $\bar{\lambda}-mean$ wave length of quasi monochromatic wave in vacuum, $n-$ refrective index of the medium.

The number of photons N emitted during the time interval dt through an area dA within a solid angle $d\Omega$ by a source of specific intensity K is given by

54

Appendix 2 (Continued)

$$Nhv = K(v)dvdtdAd\Omega \tag{5}$$

The principal intensity x is given by

$$x = K(v)dvd\Omega \tag{6}$$

The effective area dA of principal wave is given by

$$dA = \left(\frac{\lambda}{2n\,sin\theta}\right)^2 \tag{7}$$

where $n\,sin\theta$ is the numerical aperture of the lens system.

From the equations (5), (6) and (7) the number of photons N per principal

wave can be obtained.

$$N = \left(\frac{\lambda}{2}\right)^2 \frac{X}{n^2}\frac{dt}{sin^2\theta\,v} \tag{8}$$

Using equation (4)

$$\frac{N}{g} = mean\ occupation\ number = \frac{x\lambda^2\tau_c}{sin^2\theta hvn^2} \tag{9}$$

The coherence time

$$\tau_c = \frac{1}{dv}$$

Inserting this value for mean occupation number in equation (1) the thermodynamic

entropy S_x of the principal wave can be obtained.

$$S_X = \frac{kdt}{4\tau_c}\left[\left(1 + \frac{\lambda^2 X\tau_c}{hvn^2 sin^2\theta}\right)log\left(1 + \frac{\lambda^2 X\tau_c}{hvn^2 sin^2\theta}\right) - \frac{\lambda^2 X\tau_c}{hvn^2 sin^2\theta}log\frac{\lambda^2 X\tau_c}{hvn^2 sin^2\theta}\right] \tag{10}$$

Since the principal waves are statistically independent, the thermodynamic entropy of

a given partially coherent wave field can be calculated by adding the entropies of all

the principal waves.

$$S = \sum_{j=-\infty}^{+\infty} S_X = \frac{kdt}{4\tau_c}\sum_{j=-\infty}^{+\infty}\left[\left(1 + \frac{\lambda^2 X_j\tau_c}{hvn^2 sin^2\theta}\right)log\left(1 + \frac{\lambda^2 X_j\tau_c}{hvn^2 sin^2\theta}\right) - \frac{\lambda^2 X_j\tau_c}{hvn^2 sin^2\theta}log\frac{\lambda^2 X_j\tau_c}{hvn^2 sin^2\theta}\right] \tag{11}$$

55

Appendix 3 License Agreement

ELSEVIER LICENSE
TERMS AND CONDITIONS

Nov 28, 2012

This is a License Agreement between Samantha Wijewardane ("You") and Elsevier ("Elsevier") provided by Copyright Clearance Center ("CCC"). The license consists of your order details, the terms and conditions provided by Elsevier, and the payment terms and conditions.

All payments must be made in full to CCC. For payment instructions, please see information listed at the bottom of this form.

Supplier Elsevier Limited The Boulevard,Langford Lane Kidlington,Oxford,OX5 1GB,UK

Registered Company Number 1982084

Customer name Samantha Wijewardane

Customer address

License number 3030980115908

License date Nov 16, 2012

Licensed content publisher Elsevier

Licensed content publication Energy

Licensed content title Exergy of partially coherent thermal radiation

Licensed content author S. Wijewardane,Yogi Goswami

Licensed content date June 2012

Licensed content volume number 42

Licensed content issue number 1

Number of pages 6

Start Page 497

End Page 502

Type of Use reuse in a thesis/dissertation

Intended publisher of new work other

56

Appendix 3 (Continued)

Portion full article

Format both print and electronic

Are you the author of this Elsevier article? Yes

Will you be translating? No

Order reference number

Title of your thesis/dissertation

Assessment of methods to manipulate thermal emission and evaluate the quality of thermal radiation for direct energy conversion

Expected completion date Nov 2012

Estimated size (number of pages) 80

Elsevier VAT number GB 494 6272 12

Supplier Elsevier Limited The Boulevard,Langford Lane Kidlington,Oxford,OX5 1GB,UK

Registered Company Number   1982084

Customer name   Samantha Wijewardane

Customer address

License number   3030971335477

License date   Nov 16, 2012

Licensed content publisher   Elsevier

Licensed content publication   Renewable and Sustainable Energy Reviews

Licensed content title   A review on surface control of thermal radiation by paints and coatings for   new energy applications

Licensed content author   S. Wijewardane,D.Y. Goswami

Licensed content date May 2012

Licensed content volume number 16

Licensed content issue number 4

Number of pages 11

Appendix 3 (Continued)

Start Page 1863

End Page 1873

Type of Use reuse in a thesis/dissertation

Portion full article

Format electronic

Are you the author of this Elsevier article? Yes

Will you be translating? No

Order reference number

Title of your thesis/dissertation

Assessment of methods to manipulate thermal emission and evaluate the quality of thermal radiation for direct energy conversion

Expected completion date Nov 2012

Estimated size (number of pages) 80

Elsevier VAT number GB 494 6272 12

Permissions price

0.00 USD

VAT/Local Sales Tax

0.0 USD / 0.0 GBP

Total

0.00 USD

Terms and Conditions

INTRODUCTION

1. The publisher for this copyrighted material is Elsevier. By clicking "accept" in connection with completing this licensing transaction, you agree that the following terms and conditions apply to this transaction (along with the Billing and Payment terms and conditions established by Copyright Clearance Center, Inc. ("CCC"), at the time that you opened your Rightslink account and that are available at any time at http://myaccount.copyright.com).

Appendix 3 (Continued)

GENERAL TERMS

2. Elsevier hereby grants you permission to reproduce the aforementioned material subject to the terms and conditions indicated.

3. Acknowledgement: If any part of the material to be used (for example, figures) has appeared in our publication with credit or acknowledgement to another source, permission must also be sought from that source. If such permission is not obtained then that material may not be included in your publication/copies. Suitable acknowledgement to the source must be made, either as a footnote or in a reference list at the end of your publication, as follows:

"Reprinted from Publication title, Vol /edition number, Author(s), Title of article / title of chapter, Pages No., Copyright (Year), with permission from Elsevier [OR APPLICABLE SOCIETY COPYRIGHT OWNER]." Also Lancet special credit - "Reprinted from The Lancet, Vol. number, Author(s), Title of article, Pages No., Copyright (Year), with permission from Elsevier."

4. Reproduction of this material is confined to the purpose and/or media for which permission is hereby given.

5. Altering/Modifying Material: Not Permitted. However figures and illustrations may be altered/adapted minimally to serve your work. Any other abbreviations, additions, deletions and/or any other alterations shall be made only with prior written authorization of Elsevier Ltd. (Please contact Elsevier at permissions@elsevier.com)

6. If the permission fee for the requested use of our material is waived in this instance, please be advised that your future requests for Elsevier materials may attract a fee.

7. Reservation of Rights: Publisher reserves all rights not specifically granted in the combination of (i) the license details provided by you and accepted in the course of this licensing transaction, (ii) these terms and conditions and (iii) CCC's Billing and Payment terms and conditions.

8. License Contingent Upon Payment: While you may exercise the rights licensed immediately upon issuance of the license at the end of the licensing process for the transaction, provided that you have disclosed complete and accurate details of your proposed use, no license is finally effective unless and until full payment is received from you (either by publisher or by CCC) as provided in CCC's Billing and Payment terms and conditions. If full payment is not received on a timely basis, then any license preliminarily granted shall be deemed automatically revoked and shall be void as if never granted. Further, in the event that you breach any of these terms and conditions or any of CCC's Billing and Payment terms and conditions, the license is automatically revoked and shall be void as if never granted. Use of materials as described in a revoked license, as well as any use of the materials beyond the scope of an unrevoked license, may constitute copyright infringement and publisher reserves the right to take any and all action to protect its copyright in the materials.

Appendix 3 (Continued)

9. Warranties: Publisher makes no representations or warranties with respect to the licensed material.

10. Indemnity: You hereby indemnify and agree to hold harmless publisher and CCC, and their respective officers, directors, employees and agents, from and against any and all claims arising out of your use of the licensed material other than as specifically authorized pursuant to this license.

11. No Transfer of License: This license is personal to you and may not be sublicensed, assigned, or transferred by you to any other person without publisher's written permission.

12. No Amendment Except in Writing: This license may not be amended except in a writing signed by both parties (or, in the case of publisher, by CCC on publisher's behalf).

13. Objection to Contrary Terms: Publisher hereby objects to any terms contained in any purchase order, acknowledgment, check endorsement or other writing prepared by you, which terms are inconsistent with these terms and conditions or CCC's Billing and Payment terms and conditions. These terms and conditions, together with CCC's Billing and Payment terms and conditions (which are incorporated herein), comprise the entire agreement between you and publisher (and CCC) concerning this licensing transaction. In the event of any conflict between your obligations established by these terms and conditions and those established by CCC's Billing and Payment terms and conditions, these terms and conditions shall control.

14. Revocation: Elsevier or Copyright Clearance Center may deny the permissions described in this License at their sole discretion, for any reason or no reason, with a full refund payable to you. Notice of such denial will be made using the contact information provided by you. Failure to receive such notice will not alter or invalidate the denial. In no event will Elsevier or Copyright Clearance Center be responsible or liable for any costs, expenses or damage incurred by you as a result of a denial of your permission request, other than a refund of the amount(s) paid by you to Elsevier and/or Copyright Clearance Center for denied permissions.

LIMITED LICENSE

The following terms and conditions apply only to specific license types:

15. **Translation**: This permission is granted for non-exclusive world **English** rights only unless your license was granted for translation rights. If you licensed translation rights you may only translate this content into the languages you requested. A professional translator must perform all translations and reproduce the content word for word preserving the integrity of the article. If this license is to re-use 1 or 2 figures then permission is granted for non-exclusive world rights in all languages.

60

Appendix 3 (Continued)

16. **Website**: The following terms and conditions apply to electronic reserve and author websites:**Electronic reserve**: If licensed material is to be posted to website, the web site is to be password-protected and made available only to bona fide students registered on a relevant course if:

This license was made in connection with a course,

This permission is granted for 1 year only. You may obtain a license for future website posting,

All content posted to the web site must maintain the copyright information line on the bottom of each image,

A hyper-text must be included to the Homepage of the journal from which you are licensing athttp://www.sciencedirect.com/science/journal/xxxxx or the Elsevier homepage for books athttp://www.elsevier.com , and

Central Storage: This license does not include permission for a scanned version of the material to be stored in a central repository such as that provided by Heron/XanEdu.

17. **Author website** for journals with the following additional clauses:

All content posted to the web site must maintain the copyright information line on the bottom of each image, and the permission granted is limited to the personal version of your paper. You are not allowed to download and post the published electronic version of your article (whether PDF or HTML, proof or final version), nor may you scan the printed edition to create an electronic version. A hyper-text must be included to the Homepage of the journal from which you are licensing athttp://www.sciencedirect.com/science/journal/xxxxx . As part of our normal production process, you will receive an e-mail notice when your article appears on Elsevier's online service ScienceDirect (www.sciencedirect.com). That e-mail will include the article's Digital Object Identifier (DOI). This number provides the electronic link to the published article and should be included in the posting of your personal version. We ask that you wait until you receive this e-mail and have the DOI to do any posting.

Central Storage: This license does not include permission for a scanned version of the material to be stored in a central repository such as that provided by Heron/XanEdu.

18. **Author website** for books with the following additional clauses:
Authors are permitted to place a brief summary of their work online only.
A hyper-text must be included to the Elsevier homepage at http://www.elsevier.com .
All content posted to the web site must maintain the copyright information line on the bottom of each image. You are not allowed to download and post the published electronic version of your chapter, nor may you scan the printed edition to create an electronic version.Central Storage: This license does not include permission for a scanned version of the material to be stored in a central repository such as that provided by Heron/XanEdu.

19. **Website** (regular and for author): A hyper-text must be included to the Homepage of the journal from which you are licensing at http://www.sciencedirect.com/science/journal/xxxxx. or for books to the Elsevier homepage at http://www.elsevier.com

Appendix 3 (Continued)

20. **Thesis/Dissertation**: If your license is for use in a thesis/dissertation your thesis may be submitted to your institution in either print or electronic form. Should your thesis be published commercially, please reapply for permission. These requirements include permission for the Library and Archives of Canada to supply single copies, on demand, of the complete thesis and include permission for UMI to supply single copies, on demand, of the complete thesis. Should your thesis be published commercially, please reapply for permission.

21. **Other Conditions**:

v1.6